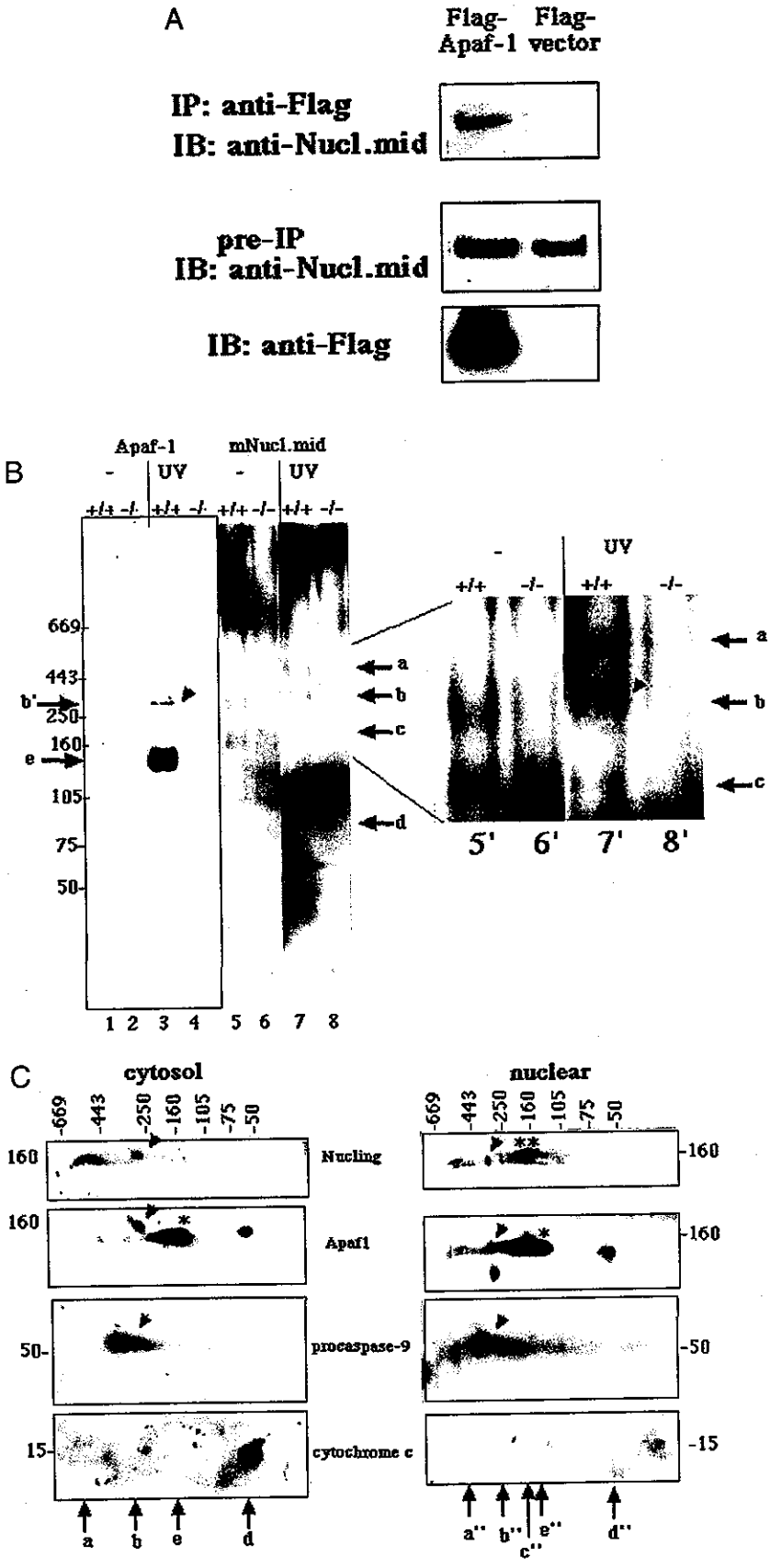


FIG. 7. **Nucling assembles with Apaf-1 and pro-caspase-9.** *A*, Nucling interacts with Apaf-1. COS7 cells were transfected with the indicated expression vector (*Flag-Apaf-1* or *Flag-vector*). After 18 h, cellular lysates were prepared and incubated with the anti-Flag antibody for immunoprecipitation (*IP*). Immunoprecipitates were subjected to immunoblotting (*IB*) using anti-Nucling antibody (*anti-Nucl.mid*). *upper panel*, expression levels of endogenous Nucling in preimmunoprecipitated (*pre-IP*) cellular lysates were confirmed by IB with anti-Nucl.mid antibody (*middle panel*). Expression of Flag-Apaf-1 was confirmed by IB with anti-Flag antibody (*lower panel*). *B*, several Nucling-containing complexes or Apaf-1-containing complexes were observed in UV-irradiated WT MEFs but not in Nucling$^{-/-}$ MEFs on native gel electrophoresis. Fifty $\mu$g of the cytosol fraction was subjected to nondenaturing electrophoresis (first dimension). Proteins were transferred and immunoblotted with an anti-Nucl.mid antibody for Nucling or anti-Apaf-1 antibody. *Arrows* indicate the prominent Nucling (*a–d*) or Apaf-1 (*b'* and *e*)-containing bands. The *right panel* (*lane 5'* to *lane 8'*) is an enlarged image of part of the *left panel* ranging from *lane 5* to *lane 8*. A common complex band of ~260 kDa in *lanes 3* and *7'* is marked with *arrowheads*. *C*, apoptosome components were assembled in the complex containing Nucling. Cytosol and nuclear fractions were analyzed as the second dimension. Immunoblot of the second-dimension gel of cytosol or nuclear protein complexes from the UV-irradiated WT MEFs revealed the presence of Nucling (160 kDa), Apaf-1 (120 kDa), and pro-caspase-9 (50 kDa) in a protein complex of ~260 kDa in the native first-dimension gel (*lanes b* and *b'*, marked with *arrowheads*). A band of putative free Apaf-1(*) or free Nucling (**) is marked with *asterisks*. *Arrows a–e* and *a''–e''* correspond to *arrows a–e* of *B*, respectively.

indicate that cytochrome *c* is released from Apaf-1 at the time of nuclear translocation.

As described previously, Nucling$^{-/-}$ mice displayed frequent inflammatory lesions (9) but no other defects similar to those of Apaf-1$^{-/-}$ or caspase-9$^{-/-}$ mice, including forebrain hyperplasia (11, 30, 31). Although this phenotypic discrepancy might come from the existence of unknown redundant molecules or pathways, and Nucling may not be essential for apoptosis during neural development, we observed distinct differences between WT and Nucling$^{-/-}$ mice concerning the apoptotic

responsiveness under cellular stress. In particular, the expression levels of Apaf-1, cytochrome *c*, and caspase-9 in MEF cells under several forms of cellular stress differed strikingly between WT and Nucling$^{-/-}$ strains. In fact, down-regulation of Apaf-1 was also observed in several Nucling$^{-/-}$ tissues including kidney, spleen, and lung but not in brain (data not shown). There might be an alternative molecule(s) in place of Nucling in the brain or neural development. There might also be a distinct signal transduction pathway for stress-induced apoptosis, different from that for developmental apoptosis. Or other apoptosome-independent mitochondrial apoptosis-inducing factors, such as AIF or endonuclease G, may be prominent in the development of Nucling$^{-/-}$ mice. Actually, it has been reported that there must be an Apaf-1-independent pathway for apoptosis triggered by cytotoxic stress (32–34). Our findings may also support the hypothesis that the "regulation of Apaf-1 expression may be a new regulatory mechanism developed in postmitotic cells to prevent an irreversible commitment to die after the release of cytochrome *c*", proposed by Sanchis *et al.* (34) recently.

We reported previously that Nucling negatively regulated the antiapoptotic molecule galectin-3 and NF-κB activation (9). NF-κB is known to be most commonly involved in suppressing apoptosis by transactivating the expression of antiapoptotic genes (35). From these findings, we concluded that a stress-induced factor, Nucling, promotes apoptosis by regulating three pathways, apoptosome up-regulation, galectin-3 down-regulation, and NF-κB inactivation.

This report shows that Nucling is the regulator of Apaf-1 expression and plays an important role in the regulation of stress-induced apoptosis.

*Acknowledgments*—We thank K. Ikuta and T. Honjo for providing a 129/Sv mouse genomic library. We are grateful to M. Shono for assistance with confocal microscopy; M. Nakatani, M. Matsui, S. Fujihara, K. Moriyama, and Y. Hayashi for whole mount *in situ* hybridization; and S. Okamura and N. Yamakawa for flow cytometry analyses. Use of the image analysis and biotechnology facilities was made possible by core grants to the Instrument Center, The University of Tokushima, School of Medicine. We also thank K. Tsuchida, K. Yamashita, F. Nasu, A. Hirao, and R. Hakem for helpful comments.

REFERENCES

1. White, E. (1996) *Genes Dev.* **10,** 1–15
2. Wyllie, A. H., Kerr, J. F., and Currie, A. R. (1980) *Int. Rev. Cytol.* **68,** 251–306
3. Steller, H. (1995) *Science* **267,** 1445–1449
4. Huang, D. C., and Strasser, A. (2000) *Cell* **103,** 839–842
5. Wang, X. (2001) *Genes Dev.* **15,** 2922–2933
6. Sakai, T., Liu, L., Shishido, Y., and Fukui, K. (2003) *J Biochem. (Tokyo)* **133,** 429–436
7. Welch, A. Y., and Herman, I. M. (2002) *Int. J. Biochem. Cell Biol.* **34,** 864–881
8. Shuster, C. B., Lin, A. Y., Nayak, R., and Herman, I. M. (1996) *Cell Motil. Cytoskeleton* **35,** 175–187
9. Liu, L., Sakai, T., Sano, N., and Fukui, K. (2004) *Biochem. J.* **380,** 31–41
10. Yu, F., Finley, R. L., Jr., Raz, A., and Kim, H. R. (2002) *J. Biol. Chem.* **277,** 15819–15827
11. Hakem, R., Hakem, A., Duncan, G. S., Henderson, J. T., Woo, M., Soengas, M. S., Elia, A., de la Pompa, J. L., Kagi, D., Khoo, W., Potter, J., Yoshida, R., Kaufman, S. A., Lowe, S. W., Penninger, J. M., and Mak, T. W. (1998) *Cell* **94,** 339–352
12. Honarpour, N., Gilbert, S. L., Lahn, B. T., Wang, X., and Herz, J. (2001) *Proc. Natl. Acad. Sci. U. S. A.* **98,** 9683–9687
13. Hansen, W. J., Cowan, N. J., and Welch, W. J. (1999) *J. Cell Biol.* **145,** 265–277
14. Kimura, H., Minakami, H., Sekiguchi, I., Otsuki, K., and Shoji, A. (1999) *J Biochem. (Tokyo)* **126,** 340–346
15. Li, P., Nijhawan, D., Budihardjo, I., Srinivasula, S. M., Ahmad, M., Alnemri, E. S., and Wang, X. (1997) *Cell* **91,** 479–489
16. Zou, H., Henzel, W. J., Liu, X., Lutschg, A., and Wang, X. (1997) *Cell* **90,** 405–413
17. Ruiz-Vela, A., Gonzalez de Buitrago, G., and Martinez, A. C. (2002) *FEBS Lett.* **517,** 133–138
18. Du, C., Fang, M., Li, Y., Li, L., and Wang, X. (2000) *Cell* **102,** 33–42
19. Krajewski, S., Krajewska, M., Ellerby, L. M., Welsh, K., Xie, Z., Deveraux, Q. L., Salvesen, G. S., Bredesen, D. E., Rosenthal, R. E., Fiskum, G., and Reed, J. C. (1999) *Proc. Natl. Acad. Sci. U. S. A.* **96,** 5752–5757
20. Li, L. Y., Luo, X., and Wang, X. (2001) *Nature* **412,** 95–99
21. Liu, X., Kim, C. N., Yang, J., Jemmerson, R., and Wang, X. (1996) *Cell* **86,** 147–157
22. Samali, A., Cai, J., Zhivotovsky, B., Jones, D. P., and Orrenius, S. (1999) *EMBO J.* **18,** 2040–2048
23. Susin, S. A., Lorenzo, H. K., Zamzami, N., Marzo, I., Snow, B. E., Brothers, G. M., Mangion, J., Jacotot, E., Costantini, P., Loeffler, M., Larochette, N., Goodlett, D. R., Aebersold, R., Siderovski, D. P., Penninger, J. M., and Kroemer, G. (1999) *Nature* **397,** 441–446
24. Susin, S. A., Lorenzo, H. K., Zamzami, N., Marzo, I., Brenner, C., Larochette, N., Prevost, M. C., Alzari, P. M., and Kroemer, G. (1999) *J. Exp. Med.* **189,** 381–394
25. Verhagen, A. M., Ekert, P. G., Pakusch, M., Silke, J., Connolly, L. M., Reid, G. E., Moritz, R. L., Simpson, R. J., and Vaux, D. L. (2000) *Cell* **102,** 43–53
26. Jia, L., Srinivasula, S. M., Liu, F. T., Newland, A. C., Fernandes-Alnemri, T., Alnemri, E. S., and Kelsey, S. M. (2001) *Blood* **98,** 414–421
27. Wolf, B. B., Schuler, M., Li, W., Eggers-Sedlet, B., Lee, W., Tailor, P., Fitzgerald, P., Mills, G. B., and Green, D. R. (2001) *J. Biol. Chem.* **276,** 34244–34251
28. Porter, A. G. (1999) *Trends Cell Biol.* **9,** 394–401
29. Ritter, P. M., Marti, A., Blanc, C., Baltzer, A., Krajewski, S., Reed, J. C., and Jaggi, R. (2000) *Eur. J. Cell Biol.* **79,** 358–364
30. Yoshida, H., Kong, Y. Y., Yoshida, R., Elia, A. J., Hakem, A., Hakem, R., Penninger, J. M., and Mak, T. W. (1998) *Cell* **94,** 739–750
31. Cecconi, F., Alvarez-Bolado, G., Meyer, B. I., Roth, K. A., and Gruss, P. (1998) *Cell* **94,** 727–737
32. McDonnell, M. A., Wang, D., Khan, S. M., Vander Heiden, M. G., and Kelekar, A. (2003) *Cell Death Differ.* **10,** 1005–1015
33. Belmokhtar, C. A., Hillion, J., Dudognon, C., Fiorentino, S., Flexor, M., Lanotte, M., and Segal-Bendirdjian, E. (2003) *J. Biol. Chem.* **278,** 29571–29580
34. Sanchis, D., Mayorga, M., Ballester, M., and Comella, J. X. (2003) *Cell Death Differ.* **10,** 977–986
35. Kucharczak, J., Simmons, M. J., Fan, Y., and Gelinas, C. (2003) *Oncogene* **22,** 8961–8982

# Nucling mediates apoptosis by inhibiting expression of galectin-3 through interference with nuclear factor κB signalling

Li LIU*, Takashi SAKAI*, Nobuya SANO† and Kiyoshi FUKUI*[1]

*The Institute for Enzyme Research, The University of Tokushima, 3-18-15 Kuramoto-Cho, Tokushima, 770-8503, Japan, and †University Hospital, The University of Tokushima, 3–18–15 Kuramoto-Cho, Tokushima, 770-8503, Japan

Nucling is a novel apoptosis-associated molecule, which is involved with cytochrome *c*/Apaf-1/caspase-9 apoptosome induction following pro-apoptotic stress. In the present study, we show first that Nucling is able to interact with galectin-3. Galectin-3 is known to participate in many biological processes, including apoptotic cell death. Nucling was found to down-regulate the expression level of galectin-3 mRNA/protein. Nucling-deficient cells, in which galectin-3 expression is up-regulated, appeared to be resistant to some forms of pro-apoptotic stress as compared with wild-type cells. In addition, the preputial gland from Nucling-deficient mice expressed a significant level of galectin-3 and exhibited a high incidence of inflammatory lesions, indicating that Nucling plays a crucial role in the homoeostasis of this gland by interacting with the galectin-3 molecule and regulating the expression level of galectin-3. Up-regulation of galectin-3 was also observed in the heart, kidney, lung, testis and ovary of the Nucling-deficient mice. In order to confirm the functional interaction between Nucling and galectin-3, a well-documented candidate for the mediator of galectin-3 expression, NF-κB (nuclear factor κB), was investigated as well. Nucling was shown to interfere with NF-κB activation via the nuclear translocation process of NF-κB/p65, thus inhibiting the expression of galectin-3. Taken together, we propose that Nucling mediates apoptosis by interacting and inhibiting expression of galectin-3.

Key words: anoikis, apoptosis, galectin-3, Nucling, nuclear factor κB (NF-κB), preputial gland.

## INTRODUCTION

Nucling is a novel protein isolated originally from murine embryonal carcinoma cells that is up-regulated during cardiac muscle differentiation [1]. cDNA for mouse Nucling encodes a polypeptide of 1411 amino acids, containing an ankyrin repeat, an aspartyl protease motif, a leucine zipper motif and two t-SNARE (target membrane soluble *N*-ethylmaleimide-sensitive fusion protein attachment protein receptor) coiled-coil domains. Nucling mRNA is expressed in various adult tissues. Nucling protein localizes in the cytoplasm, especially around the nuclear membrane in mammalian cells. Moreover, the expression level of the Nucling gene transcript increases progressively during the early developmental stages in mice, and specifically at cardiomuscular differentiation *in vitro* and *in vivo* [1]. We have recently confirmed that several apoptotic signals can induce endogenous Nucling expression. Moreover, Nucling can induce cytochrome *c* release, followed by apoptosis in mammalian cells. It was also shown that Nucling recruits the Apaf-1–pro-caspase-9 complex for the induction of apoptosis following pro-apoptotic stress (T. Sakai, L. Liu, R. Mukai-Sakai, X. C. Teng, T. Mitani, M. Matsumoto, K. Toida, K. Ishimura, Y. Shishido, T. W. Mak and K. Fukui, unpublished work). βCAP73, a novel β-actin-specific binding protein, was isolated from a bovine endothelial cell library [2], and Nucling is regarded as the mouse homologue of βCAP73 on the basis of the sequence similarity.

Galectins are a family of carbohydrate-binding proteins defined by an affinity for β-galactoside and sequence identity with the carbohydrate-binding motif [3]. The family is composed of 14 members [4]. Among them, galectin-3, the only member of chimaeric type, contains a non-lectin part connected to a carbohydrate recognition domain [4,5]. Studies have previously demonstrated that galectin-3 has a broad distribution among different tissues and cell types [6–8]. Therefore galectin-3 may play a role in a number of biological activities, such as cell–cell and cell–matrix interactions [9,10], induction of pre-mRNA splicing [11], cell cycle regulation [12], angiogenesis [13], tumorigenesis [14,15] and, more importantly, cell growth and apoptosis [16,17]. It is reported that galectin-3 ectopically expressed in a human T-cell line protected the cell from apoptosis induced by pro-apoptotic stimuli [18]. In addition, studies on galectin-3-deficient mice support further the anti-apoptotic role of galectin-3 [19]. Much remains to be learned about how galectin-3 inhibits apoptosis, although early studies have suggested the involvement of Bcl-2 [20]. One recent report showed that galectin-3 translocates to the perinuclear membrane following exposure to a variety of apoptotic stimuli, and becomes abundant in the mitochondria, where it prevents mitochondrial damage and cytochrome *c* release [21].

Recent reports provide supporting evidence that NF-κB (nuclear factor κB) and Jun are involved in the regulation of galectin-3 expression [22]. Furthermore, galectin-3-deficient mice had fewer inflammatory cells after intraperitoneal challenge with reduced levels of NF-κB activation [19]. NF-κB is activated by various stimuli, including TNF-α (tumour necrosis factor-α), interleukin-1 and lipopolysaccharide [23], and regulates the expression of genes involved in the immune response, inflammatory processes and apoptosis [24,25]. Moreover, studies on mice deficient in NF-κB subunits revealed that NF-κB has an essential role in preventing TNF-α-induced cell death [26].

Abbreviations used: EMSA, electrophoretic mobility-shift assay; H/E, haematoxylin and eosin; JIA, juvenile idiopathic arthritis; MEF, murine embryonic fibroblasts; NF-κB, nuclear factor κB; NuclingΔN, a deletion mutant of Nucling lacking the N-terminal region; RT, room temperature; RT-PCR, reverse transcriptase-PCR; TNF-α, tumour necrosis factor-α; (t-)SNARE, (target membrane) soluble *N*-ethylmaleimide-sensitive fusion protein attachment protein receptor; TUNEL, terminal deoxynucleotidyl transferase-mediated dUTP nick-end labelling; WT, wild-type.

[1] To whom correspondence should be addressed (e-mail kiyo@ier.tokushima-u.ac.jp).

In the present study, in order to investigate the signal transduction mechanism of Nucling we sought to identify Nucling-interacting proteins by screening a mouse embryo library using the yeast two-hybrid system. The result of the screening indicated positive interaction with Nucling by a galectin family member. Furthermore, we show that galectin-3 can interact with Nucling, with an up-regulated expression in several cell types or tissues of Nucling-deficient mice. We also found that NF-$\kappa$B is involved in the functional interaction between Nucling and galectin-3 expression. Finally, we propose that Nucling may mediate apoptosis by interacting and inhibiting expression of galectin-3.

## EXPERIMENTAL

### Yeast two-hybrid system

A cDNA (1.5 kb) fragment encoding the C-terminus of Nucling was inserted into pGBKT7-GAL4 (ClonTech) to generate pGBKT7-GAL4–NuclingΔN (where 'NuclingΔN' represents a deletion mutant lacking the N-terminal region) as 'bait' (a tectonic schematic representation of this is shown in Figure 1A, together with that of Nucling [1]). As shown in Figure 1(A), full-length Nucling protein consists of several potential domains for protein–protein interaction, such as two t-SNARE coiled-coil domains, an ankyrin repeat and a leucine zipper motif. In order to circumvent this complexity of interacting domains, we first selected the C-terminal fragment of cDNA as bait, which contains only one t-SNARE coiled-coil domain and covers almost half of the full-length sequence. After verification of the sequence, AH109 yeast cells were sequentially transformed with pGBKT7-GAL4–NuclingΔN and a 17.5-day mouse embryo cDNA library ($2.0 \times 10^8$ colony-forming units $\cdot$ ml$^{-1}$) in pACT (ClonTech). Selection was carried out by growth on SD/− Trp, SD/− Leu − Trp and SD/ $\alpha$-X-gal − Ade − His − Leu − Trp plates (where X-gal represents 5-bromo-4-chloroindol-3-yl $\beta$-D-galactopyranoside). Seventeen clones exhibiting activation of the *LacZ* reporter gene were identified by the $\beta$-galactosidase assay. These positive clones were isolated on Chroma Spin-1000 columns (ClonTech). Subsequent PCR amplification was performed using primers 5′-GTGAACTTGCGGGGTTTTTCAGTATCTACGT-3′ and 5′-CTATTCGATGATGAAGATACCCCACCAAACCC-3′ to amplify the cDNA inserts from all plasmids encoding candidate interacting proteins (the Advantage cDNA PCR kit). These proteins were sorted into groups on the basis of restriction digestion patterns. Since *Hae*III is a frequent-cutter restriction enzyme, it was used to digest the PCR product. Subsequently, a representative clone from each group was subjected to sequencing analysis. Lastly, the mini-prep DNA was transformed into *Escherichia coli* DH10B cells and purified.

### Co-immunoprecipitation assay and immunoblotting

Cos7 cells were transiently co-transfected with plasmids using Effectene® Transfection Reagent (Qiagen). Cells were harvested and lysed in a lysis buffer containing 20 mM Hepes, pH 7.5, 150 mM NaCl, 1 mM EDTA, 1 % (v/v) Triton X-100, 0.5 % (w/v) deoxycholate, 0.1 % (w/v) SDS and Complete™ protease inhibitor cocktail (Roche) at 24 h post-transfection. Cell extracts were clarified by centrifugation at 12 000 *g* for 30 min at 4 °C, and the supernatant was immunoprecipitated with anti-Flag M2 affinity gel (Sigma) by incubating overnight at 4 °C. The beads were washed five times with the lysis buffer and suspended in SDS loading buffer. Subsequently, the co-immunoprecipitated and lysate samples were subjected to an immunoblot assay with anti-Flag M2 monoclonal antibody–horseradish-peroxidase conjugate (Sigma) or c-Myc 9E10 antibody–horseradish-peroxidase conjugate (Santa Cruz Biotechnology).

### Immunofluorescence staining

Cos7 cells were plated on to Lab-Tek Chamber Slides (Nalge Nunc International, Naperville, IL, U.S.A.), transiently transfected with FLAG–Nucling and/or c-Myc–galectin-3, and cultured overnight. After a brief wash at room temperature (RT; ≈25 °C) in PBS, the cells were fixed in 3.7 % (w/v) paraformaldehyde in PBS for 15 min at RT. After several washes in PBS, the cells were immersed in PBS containing 0.2 % Triton X-100 for 5 min at RT, and washed three more times with PBS. Samples were incubated for 30 min at RT with 10 % goat serum. After three further washes, cells were incubated with FITC–anti-Flag M2 antibody (Sigma) and anti-Myc (Ab-1) antibody for 2 h at RT. After a further three washes with PBS, the coverslips were incubated with Texas Red™ (TXRD)-conjugated secondary antibodies (Southern Biotechnology Associates, Inc., Birmingham, AL, U.S.A.) or FITC–anti-mouse IgG (Zymed Laboratories, Inc., San Francisco, CA, U.S.A.) for 1 h. Lastly, coverslips were analysed and viewed under an Olympus FluoView microscope.

### Northern blot analysis

Total RNA of MEFs (murine embryonic fibroblasts) or preputial glands from Nucling$^{+/+}$ and Nucling$^{-/-}$ mice was isolated with the Isogen reagent (Nippon Gene, Tokyo, Japan), according to the manufacturer's instructions. After electrophoresis through formaldehyde-containing agarose gels, RNAs were transferred on to Hybond N$^+$ nylon membranes (Amersham Biosciences). Probes were labelled with [$\alpha$-$^{32}$P]dCTP (NEN Life Science Products, Inc.) using Ready-To-Go DNA Labelling Beads (− dCTP) (Amersham Biosciences). After hybridization overnight at 65 °C, blots were washed three times in 2 × SSC (where 1 × SSC is 0.15 M NaCl/0.015 M sodium citrate), 0.1 % SDS for 15 min (25 °C) and four times in 0.2 × SSC/0.1 % SDS for 30 min (65 °C). The blots were exposed to Kodak™ BioMax™ MS film at − 70 °C for 0.8–3 h.

### EMSA (electrophoretic mobility shift assay)

The NF-$\kappa$B oligonucleotide (5′-AGTTGAGGGGACTTTCCCAGGC-3′; Promega) was labelled with [$\gamma$-$^{32}$P]ATP (NEN Life Science Products, Inc.) using T4 polynucleotide kinase. MEF nuclear extracts (1 $\mu$g/$\mu$l) were added to 5 $\mu$l of gel shift binding buffer [20 % (v/v) glycerol/5 mM $MgCl_2$/2.5 mM EDTA/2.5 mM dithiothreitol/250 mM NaCl/50 mM Tris/HCl (pH 7.5)/0.25 mg/ml poly(dI-dC)]. For competition or gel-shift experiments, the binding was performed in the presence of 1 $\mu$l (1.75 pmol/$\mu$l) of unlabelled NF-$\kappa$B oligonucleotide or 5 $\mu$g of NF-$\kappa$B–p65 antibody (Santa Cruz Biotechnology Inc.) respectively. The mixture was incubated for 20 min on ice before addition of 1 $\mu$l of $^{32}$P-labelled NF-$\kappa$B oligonucleotide probe. The resulting complexes were resolved by electrophoresis on 4 % polyacrylamide gels. Finally, the gels were dried and analysed by autoradiography.

### RT-PCR (reverse transcriptase-PCR)

Total RNA from preputial glands was extracted from Nucling$^{+/+}$ and Nucling$^{-/-}$ mice using Isogen. cDNA synthesis was performed using a Superscript Preamplification System for First

Strand cDNA Synthesis kit (Invitrogen), according to the manufacturer's instructions. Synthetic oligonucleotide PCR primers for mouse Nucling were 5′-TGATCACCCAGGACCCGGAAGTTACC-3′ (sense) and 5′-GGTGCTCTTTGAGGGCGAGGAAGTG-3′ (antisense). A 25 $\mu$l reaction mixture containing 1 $\mu$l of cDNA sample as the template, 200 nM PCR primers, 0.2 mM dNTPs, 1 mM $MgCl_2$, and 2.5 units of AmpliTaq Gold® enzyme (Applied Biosystems, Foster City, CA, U.S.A.) in AmpliTaq Gold® buffer was subjected to amplification in a DNA thermal cycler (GeneAmp PCR system 9700, Applied Biosystems). PCR was performed for 34 cycles (95 °C, 1 min; 60 °C, 2 min; 72 °C, 2.5 min), with an initial incubation at 96 °C for 10 min, and final extension at 72 °C for 5 min. Samples (10 $\mu$l) of the amplified product were resolved by 1.2 % (w/v) agarose gel electrophoresis, and visualized by ethidium bromide staining. RT-PCR of glyceraldehyde-3-phosphate dehydrogenase served as a control.

### Immunohistochemistry

Frozen sections (10 $\mu$m thick) containing the maximum diameter of the tissue under study were subjected to immunohistochemistry. Sections were fixed with acetone, and endogenous peroxidase was quenched with 0.3 % hydrogen peroxide in methanol. Sections were subsequently incubated for 30 min with normal serum in the VECTASTAIN® ABC kit (Vector Laboratories, Burlingame, CA, U.S.A.) to block non-specific antibody binding, and exposed to biotin-conjugated anti-mouse Mac-2 monoclonal antibody (dilution 1:50) at 37 °C for 2 h. Finally, the sections were subjected to a peroxidase reaction with 3,3′-diaminobenzidine for 5 min, resulting in a brown-coloured precipitate at the antigen site. Between each step, the slides were washed four times with PBS buffer.

### TUNEL (terminal deoxynucleotidyl transferase-mediated dUTP nick-end labelling) assay

The TUNEL assay was performed on frozen sections (10 $\mu$m thick) using the TACS™ 2 TdT-Blue Label in Situ Apoptosis Detection Kit (Trevigen).

## RESULTS

### Nucling can interact with galectin-3

In search of proteins that interact with Nucling, we chose the N-terminal-region-lacking mutant NuclingΔN as 'bait' (Figure 1A) to screen a 17.5-day mouse embryo cDNA library using the yeast two-hybrid system. Out of $2.0 \times 10^8$ diploid colony-forming units screened, 17 positive colonies were detected. Nine of the seventeen candidates, including galectin-4, interacted with Nucling in immunoprecipitation assays of expressed proteins in mammalian cells. Since the galectin family, including galectin-1 and -3, are reported to be involved in apoptosis [27], we examined the possibility that galectin family members interact with Nucling. To confirm any direct interaction between Nucling and galectin-1, -3, and -4, we performed co-immunoprecipitation analysis. As shown in Figure 1(B), we observed that full-length Nucling could interact with galectin-3 and galectin-4, but not with galectin-1 (results not shown). In contrast, NuclingΔN could interact with galectin-4, but not with galectin-3.

In order to examine the subcellular localization of Nucling and galectin-3, we performed an immunofluorescence analysis of the transfected cells. As shown in Figures 1(C) and 1(D), we found that galectin-3 existed homogeneously in both the nucleus and the cytoplasm of cells, as was reported previously [8]. On the other hand, Nucling was found to be localized around the nuclear membrane, and also diffusely in cytoplasm. However, when Nucling and galectin-3 were co-transfected into COS7 cells, the immunofluorescence staining revealed that the expression profiles of Nucling and galectin-3 were mutually exclusive in cytoplasm; that is, the area where galectin-3 staining was negative corresponded to the area in the cytoplasm that was Nucling-positive (Figure 1D).

### Nucling is a negative regulator of galectin-3 by inhibiting NF-$\kappa$B activity

On the basis of the observation shown in Figures 1(C) and 1(D), we surmised that Nucling might down-regulate the expression of galectin-3. To confirm this hypothesis, we first investigated whether Nucling overexpression results in altered expression of endogenous galectin-3 at the cellular level (Figure 2A). We overexpressed full-length or mutant Nucling (NuclingΔN) in NIH-3T3 cells. Cell lysates subsequently showed that endogenous galectin-3 expression levels were obviously decreased in the Nucling-positive cell line (Figure 2A, lane 1), but did not change in the Nucling-null or mutant-transfected cell lines (Figure 2A, lanes 2–4).

On the other hand, in order to elucidate the physiological function of Nucling *in vivo*, we have produced Nucling-deficient mice generated by targeted disruption of the Nucling gene (T. Sakai, L. Liu, R. Mukai-Sakai, X. C. Teng, T. Mitani, M. Matsumoto, K. Toida, K. Ishimura, Y. Shishido, T. W. Mak and K. Fukui, unpublished work). We then evaluated the expression level of galectin-3 in Nucling-deficient cells. Primary MEFs were prepared from embryos of wild-type (WT) and mutant ($Nucling^{-/-}$) mice. Immunoblot analyses were then performed to reveal that galectin-3 expression was markedly up-regulated in the $Nucling^{-/-}$ cells (Figure 2B, lane 2) compared with WT cells (Figure 2B, lane 1). We therefore concluded that Nucling was able to inhibit the expression of galectin-3.

Anoikis is the name given to a special form of cell death, namely detachment-induced cell death or suspension-induced apoptosis. Galectin-3 is reported to be able to protect human breast epithelial cells against apoptosis induced by anoikis [9]. There is also evidence that galectin-3 prevents mitochondrial damage and cytochrome *c* release [21,28]. Nucling is shown to induce cytochrome *c* release following pro-apoptotic stress (T. Sakai, L. Liu, R. Mukai-Sakai, X. C. Teng, T. Mitani, M. Matsumoto, K. Toida, K. Ishimura, Y. Shishido, T. W. Mak and K. Fukui, unpublished work). To determine whether galectin-3 is regulated by Nucling during the stress of anoikis or $H_2O_2$-induced apoptosis, we compared the expression levels of galectin-3 in two genotypes, WT ($Nucling^{+/+}$) and $Nucling^{-/-}$ cells. The protein expression level of galectin-3 was significantly higher in the Nucling-deficient group than in WT, both in the absence and presence of pro-apoptotic stress (Figure 2B, lanes 3–6). The RNA expression of galectin-3 was also up-regulated in $Nucling^{-/-}$ MEFs relative to that in $Nucling^{+/+}$ cells, and further enhancement of the up-regulation was observed in both cell lines under conditions of anoikis and $H_2O_2$ exposure (Figure 2C, land 3–6). Nucling is therefore considered to be a negative regulator of galectin-3 expression both at the RNA and the protein level.

Although it is possible that Nucling negatively regulates galectin-3 by interacting with this molecule at the protein level, it is still unclear how Nucling leads to transcriptional down-regulation of galectin-3. In order to clarify the functional interaction between Nucling and galectin-3, we postulated the possibility that additional factor(s) is (are) involved in the

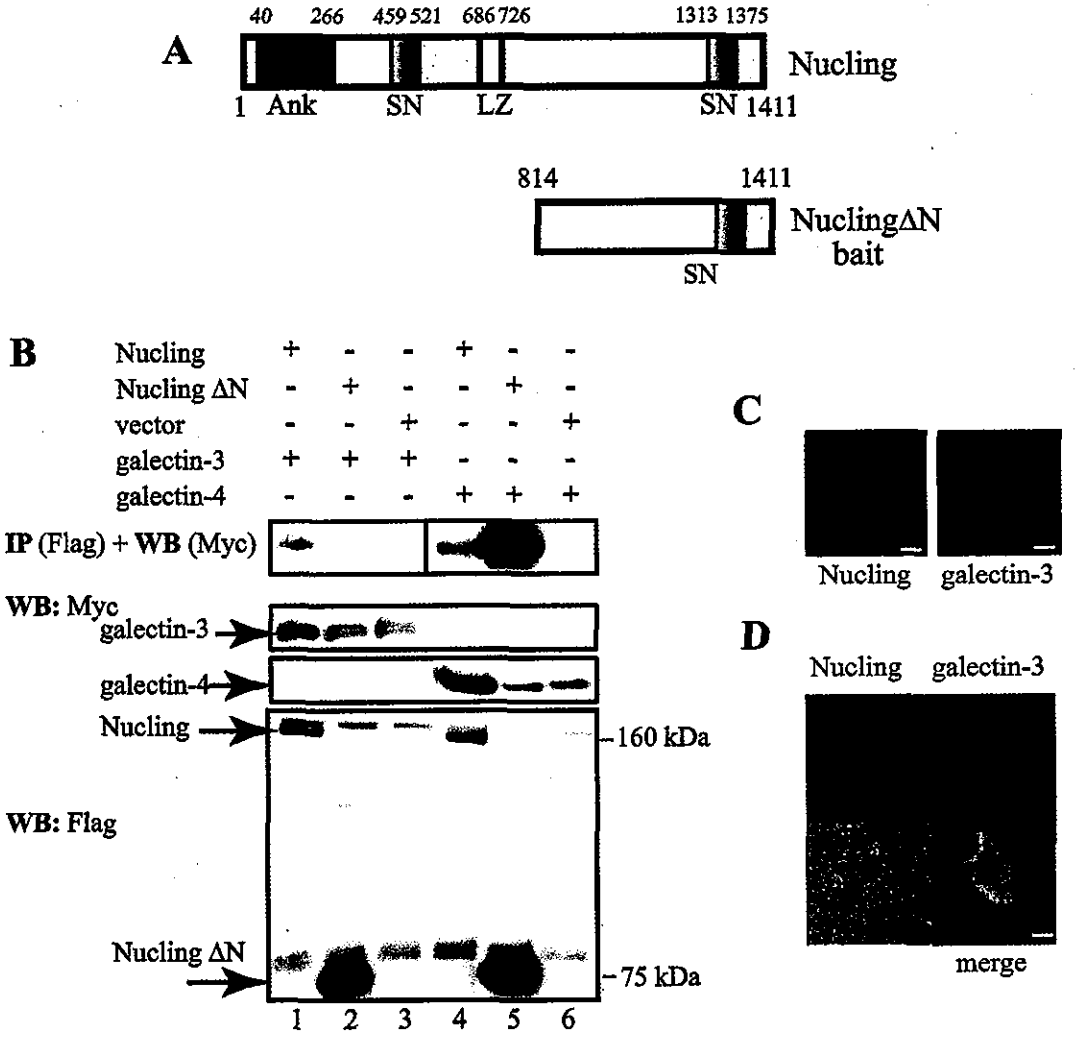


**Figure 1 Interaction of Nucling with galectin-3**

(**A**) Primary structures of the full-length Nucling and its deletion mutant (NuclingΔN; amino acids 814–1411) used as bait in a yeast two-hybrid assay are illustrated with typical motifs. Ank, SN and LZ represent ankyrin repeat region, t-SNARE coiled-coil domain and leucine zipper motif respectively. (**B**) COS-7 cells were transiently co-transfected with FLAG–Nucling/FLAG–NuclingΔN/vector and Myc–galectin-3/Myc–galectin-4. Lysates were subjected to co-immunoprecipitation assay (IP) with anti-Flag antibody. Immunoblot analysis (WB) was performed with anti-Myc antibody. The presence of galectin-3 or galectin-4 and Nucling or NuclingΔN in the same lysates were verified by immunoblotting with anti-Myc antibody and anti-FLAG antibody respectively. (**C** and **D**) Subcellular localization of transfected galectin-3 (**C**, left panel) or Nucling (**C**, right panel) alone, and co-transfected with galectin-3 and Nucling together (**D**) in COS-7 cells were analysed by subjecting cells to immunofluorescence staining. The bar represents 10 $\mu$m.

inhibition of galectin-3 expression by Nucling. We found an NF-$\kappa$B binding sequence (5′-GGGAGATCCC-3′) in the genomic sequence of Mac-2 (990–999 bp) [29], which matches completely with the consensus $\kappa$B recognition sequence (5′-GGG-RNNYYCC-3′).

This observation led us to examine and compare the level of NF-$\kappa$B between WT and Nucling-deficient MEFs. Immunoblot analysis of nuclear and cytoplasmic proteins revealed that the NF-$\kappa$B–p65 protein level was markedly higher in the nuclear fraction of Nucling$^{-/-}$ MEFs (Figure 2D, lane 1) than in that of Nucling$^{+/+}$ MEFs (lane 2), but in the cytosolic fraction no obvious difference was observed (lanes 3 and 4).

Furthermore, in order to investigate the capacity of proteins from nuclear extracts of Nucling$^{+/+}$ and Nucling$^{-/-}$ MEFs to interact with oligonucleotides containing a consensus binding sequence for NF-$\kappa$B, EMSA was performed (Figure 2E). The results from the gel-shift study showed that the DNA-binding capacity of one of the NF-$\kappa$B complexes from Nucling$^{-/-}$ MEF nuclear extracts was increased compared with that from Nucling$^{+/+}$ MEFs (Figure 2E, lanes 2 and 3, arrow A). Addition of an antibody specific for the p65 subunit of NF-$\kappa$B clearly attenuated this DNA-binding activity (Figure 2E, lanes 4 and 5, arrow A). To confirm the specificity of NF-$\kappa$B binding in this assay, a non-labelled NF-$\kappa$B oligonucleotides probe was used as competitor. As shown in *Figure 2(E)*, lanes 6 and 7, non-labelled probe was able to compete for the binding of two complexes (shown by arrows A and B), indicating the formation of p65–p50 (arrow A) and p50–p50 (arrow B) complexes in this assay. Taken together, these results indicate that Nucling might inhibit NF-$\kappa$B activity by interfering with the nuclear translocation of NF-$\kappa$B–p65 from the cytoplasm.

### The preputial gland of Nucling$^{-/-}$ mice exhibited inflammatory lesions

In order to examine the pathophysiological significance of Nucling at the whole animal level, we then analysed the WT

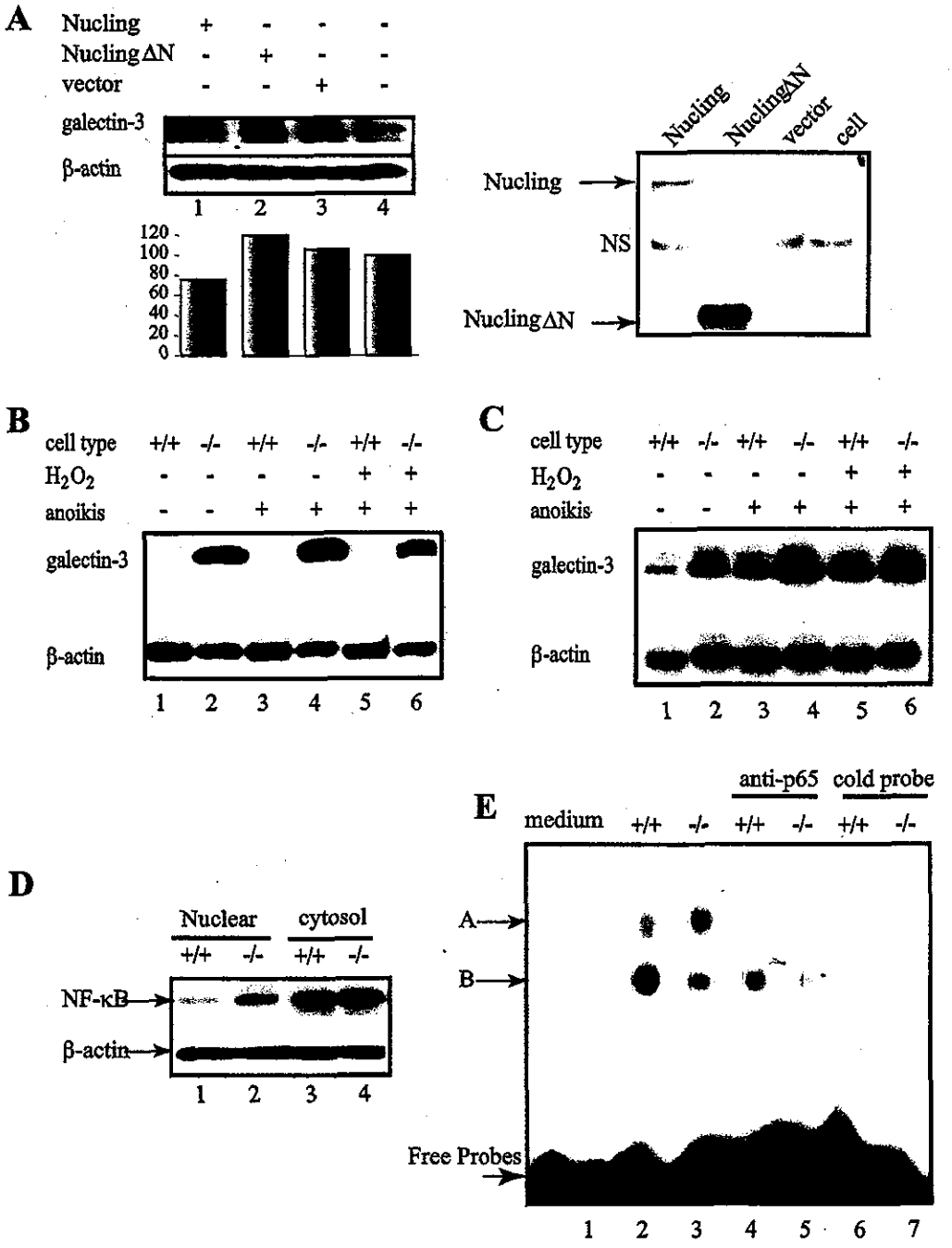


**Figure 2 Up-regulation in the level of protein and mRNA of galectin-3 in MEFs of Nucling-null mice**

(**A**) NIH3T3 cells were transiently overexpressed with Nucling, NuclingΔN or vector. Lysates were subjected to immunoblot analysis with anti-Mac2 antibody to check the level of endogenous galectin-3 (upper-left panel). The signals were scanned and calculated using NIH Image Analysis Software (lower-left panel). The presence of Nucling or NuclingΔN was revealed with anti-Flag M2 antibody (right panel). (**B**) MEFs of WT and Nucling$^{-/-}$ mice were treated with or without 0.25 % trypsin/EDTA (anoikis) and 0.8 mM $H_2O_2$ for 16 h. Then, the level of galectin-3 protein in MEFs was examined with galectin-3 antibody (Mac-2). To confirm the equal loading of the protein in each lane, the same blot was probed with β-actin antibody (Sigma). (**C**) Total RNA of MEF was isolated with Isogen from WT and Nucling$^{-/-}$ embryos, and then Northern blotting was performed with a $^{32}$P-labelled cDNA fragment of galectin-3. The same blot was probed with β-actin (ClonTech). (**D**) Translocation of NF-κB–p65 from the cytoplasm to the nucleus in Nucling$^{-/-}$ and Nucling$^{+/+}$ MEFs was examined by immunoblot analysis. Nuclear and cytosolic fraction proteins were used for determination of the NF-κB–p65 level. A monoclonal anti-NF-κB–p-65 antibody was used at a dilution of 1:500. The equal loading of the protein in each lane was confirmed by β-actin antibody. (**E**) Nuclear extracts from Nucling$^{+/+}$ and Nucling$^{-/-}$ MEFs were isolated and analysed by EMSA as described in the Experimental section.

and knock-out mice. No obvious phenotypic differences were observed initially between Nucling$^{+/+}$ and Nucling$^{-/-}$ mice. However, after the age of 4 months, apparent swellings of preputial glands were frequently observed in Nucling$^{-/-}$ mice. The preputial gland is a part of the male reproductive system, appearing as a paired structure on either side of the penis in the male mouse. This gland is reported to play an important role in the production of olfactory substances, which attract the opposite sex [30]. When mutant mice reached the age of 12 months, more than 50 % of Nucling$^{-/-}$ and 30 % of Nucling$^{+/-}$ males displayed the same symptoms, i.e. swelling of the preputial gland, under specific pathogen-free conditions (Table 1 and

**Table 1 Occurrence of swelling in male Nucling$^{-/-}$ mice**

Data show the percentage of mice with preputial gland swelling over a range of ages (15–48 weeks) for the various genotypes. The numbers in parentheses show the number of mice examined for each experiment.

| | | Proportion of mice with preputial swelling (%) | | | | | | |
|---|---|---|---|---|---|---|---|---|
| Genotype | Age (weeks) . . . | 15 | 21 | 24 | 34 | 38 | 44 | 48 |
| +/+ | | 0 (10) | 0 (10) | 0 (10) | 0 (5) | 0 (5) | 0 (5) | 0 (5) |
| +/− | | 0 (16) | 0 (16) | 0 (16) | 7.1 (14) | 12.5 (14) | 25 (10) | 37.5 (10) |
| −/− | | 3.4 (29) | 6.9 (29) | 10.3 (29) | 17.2 (29) | 29.2 (24) | 41.7 (24) | 58.3 (24) |

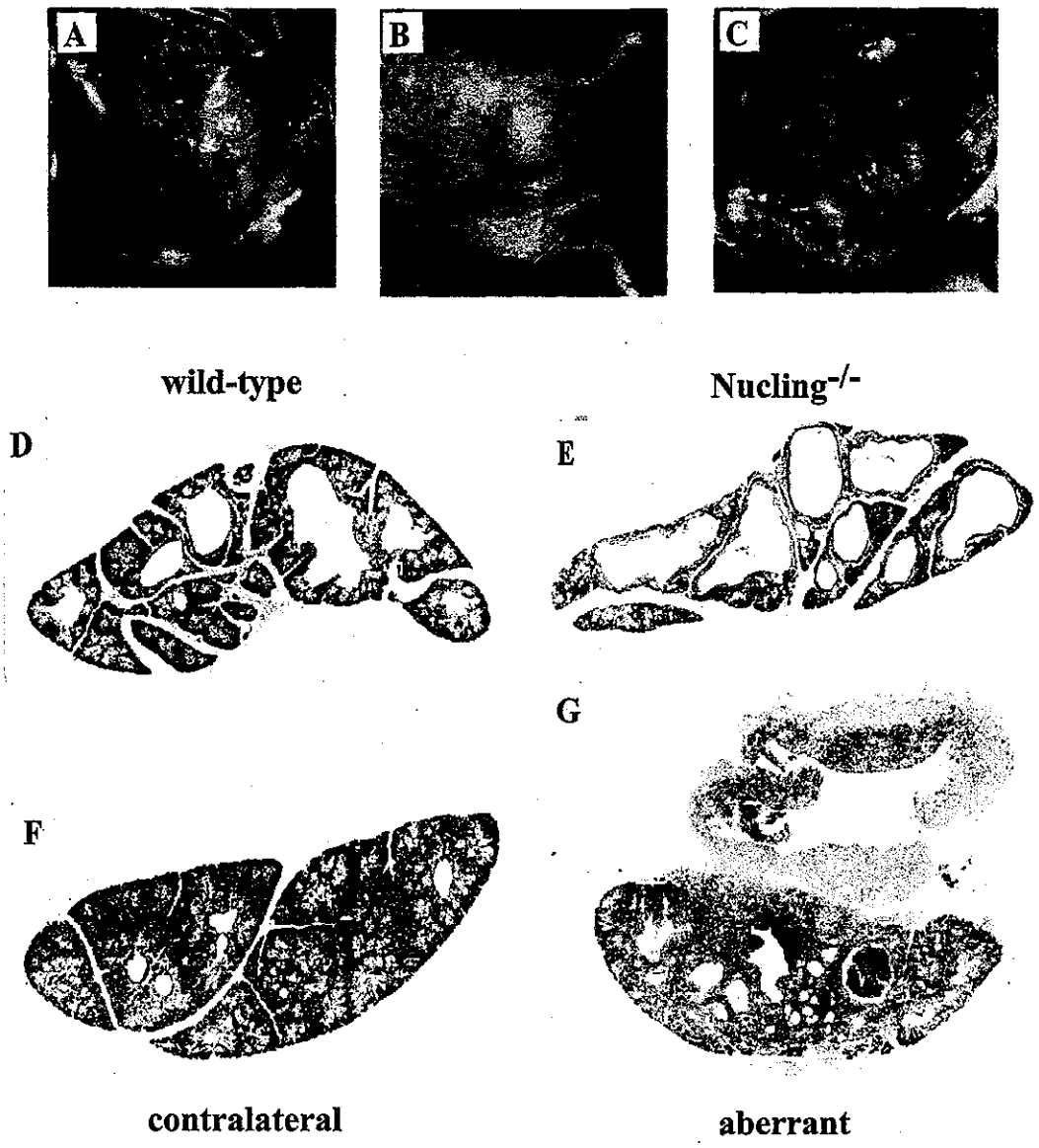


**Figure 3 Inflammatory lesions of the preputial gland of male Nucling$^{-/-}$ mice**

(**A**) Preputial gland of a 5-month-old WT male mouse after dissection. (**B**) Enlarged preputial gland (arrow) of a 5-month-old mutant male. (**C**) Aberrant preputial gland (arrow) after dissection. (**D–G**) H/E staining of paraffin-embedded sections (7 $\mu$m thick) of preputial glands from WT (**D**) and Nucling$^{-/-}$ (**E–G**) 5-month-old mice. Samples were obtained from the preputial glands of Nucling$^{-/-}$ mice without swelling (**E**), from those with swelling (**G**) and from the contralateral side (**F**).

Figures 3A–3C). The occurrence of pathological lesions was extremely high in mice with mutant allele(s) compared with their WT counterparts. Dissection of these abnormal preputial glands revealed the presence of viscous fluid in the swelling. In all the mice with abnormal glands, except one mouse with bilateral lesions, only one side of the gland was positive for swelling. Histopathological changes in the preputial gland were then analysed by H/E (haematoxylin and eosin) staining (Figures 3D–3G). On the aberrant side with the swollen preputial gland, we observed keratinization, inflammation, granulomatous

lesions, duct contraction and duct blockage (Figure 3G). In contrast, on the contralateral side of the preputial gland, we found that the number of luminal ducts was decreased, and cells were undergoing extreme hyperplasia (Figure 3F). In contrast, no marked difference could be observed between the normal-sized gland in Nucling$^{-/-}$ and that in WT mice, except for the abundant presence of luminal duct dilatation in Nucling$^{-/-}$ mice (Figures 3D and 3E). Therefore we consider that Nucling may also play a crucial role in the maintenance of the physiological function of the mouse preputial gland.

### Galectin-3 is involved in inflammatory lesions of the Nucling$^{-/-}$ preputial gland

In galectin-3-null mutant mice, galectin-3 was shown to be involved in the control of an acute inflammatory process [31]. Galectin-3 expression has also been shown to be strongly up-regulated during inflammation in acute renal failure of the rat [32], and in the presence of certain pathological conditions, such as atherosclerotic lesions, ischaemic brain lesions, JIA (juvenile idiopathic arthritis) and diabetes [33–36]. It is possible that galectin-3 is also involved in inflammatory lesions of the preputial gland. Therefore we examined first whether Nucling is expressed in the male preputial gland of WT mice by RT-PCR analysis. As shown in Figure 4(A) (lanes 1 and 3), we could detect the expression of Nucling in the preputial gland as well as in the heart. The expression level of galectin-3 in the preputial gland was then investigated in WT mice, Nucling$^{-/-}$ mice without swelling and Nucling$^{-/-}$ mice with swelling, including both the aberrant and contralateral sides, by Northern blot analysis. Galectin-3 mRNA was markedly increased in the Nucling$^{-/-}$ preputial gland as compared with the WT. Moreover, the expression of galectin-3 was significantly up-regulated on both the aberrant side and the contralateral side of Nucling$^{-/-}$ mice with swelling (Figure 4B). In contrast, we could not detect the expression of galectin-4 in the preputial gland by Northern blot analysis (Figure 4C).

### Expression of galectin-3 is up-regulated in the preputial gland of *Nucling-null* mice

To examine the localization of galectin-3 expression in the preputial gland, we then performed an immunohistochemical analysis of the gland (Figures 5A–5D). Galectin-3 was found to be negative for staining in the preputial gland of WT mice (Figure 5A). In contrast, in the preputial gland of Nucling$^{-/-}$ mice with or without swelling, galectin-3 was detected with a remarkably high level of staining around luminal ducts (Figures 5B–5D). Moreover, the expression of galectin-3 on the aberrant side of the preputial gland with swelling was much stronger, as shown in Figure 5(C). The immunostaining pattern of galectin-3 expression was in good accord with that of RNA expression (Figure 4B).

### Apoptosis is attenuated in the preputial gland of Nucling$^{-/-}$ mice

It is reported that the accumulation of inflammatory cells was mainly due to down-regulated apoptosis [35]. In order to investigate whether Nucling-induced apoptosis is involved in the inflammatory lesions in the preputial gland, we performed the TUNEL assay (Figures 6A–6D). Around the luminal ducts (Figure 6A) and in acinous tissue (results not shown) of the WT preputial gland, many TUNEL-positive cells were observed. In contrast, few TUNEL-positive cells were observed around luminal ducts in the Nucling$^{-/-}$ preputial gland (Figures 6B–6D); furthermore, TUNEL-positive cells were hardly detected in acinous tissue on the aberrant side of the preputial gland of Nucling$^{-/-}$ mice either. On the basis of this observation, we speculated that Nucling is involved in apoptosis around luminal ducts of the preputial gland. The pattern of the presence of TUNEL-positive cells is in sharp contrast with that of galectin-3 expression in Figures 5(A)–5(D). We hypothesize that down-regulation of the expression of galectin-3, through the interaction of Nucling with galectin-3, induces apoptosis around the luminal ducts.

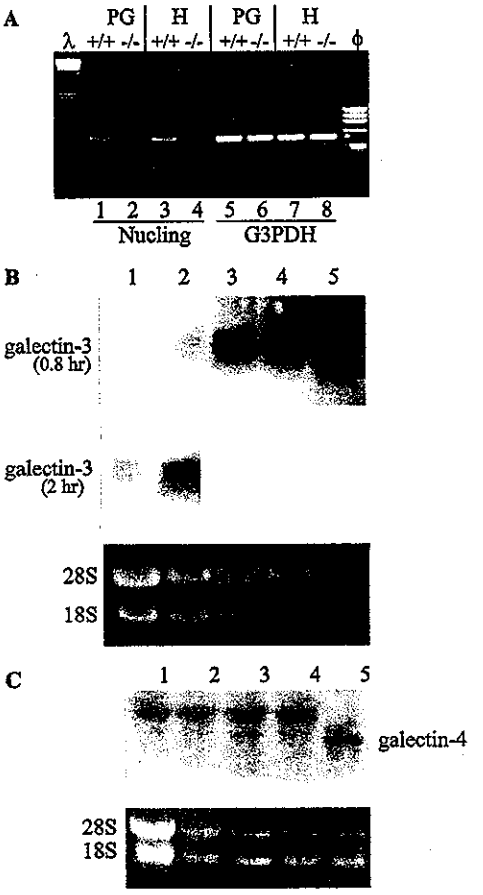


**Figure 4 Up-regulation in expression of galectin-3, but not of galectin-4, in inflammatory lesions of the preputial gland**

(**A**) Nucling expression was detected in mouse preputial gland (PG) by RT-PCR. Heart tissue (H) was used as a positive control. (**B**) Northern blot analysis of preputial gland was performed using 20 $\mu$g of total RNA from the WT preputial gland (lane 1), the Nucling$^{-/-}$ preputial gland without swelling (lane 2), the aberrant side with swelling (lane 3) and the contralateral side (lane 4). Intestine was used as a positive control (lane 5). Hybridization was performed with $^{32}$P-labelled mouse galectin-3 probe. (**C**) Northern blot analysis for galectin-4 was also performed with $^{32}$P-labelled mouse galectin-4 probe. The bottom panels in (**B**) and (**C**) show *ethidium* bromide staining of 28 S and 18 S RNA as a control for RNA loading.

### Expression of galectin-3 is generally up-regulated in tissues of Nucling-null mice

Besides the preputial gland, we also investigated the expression of galectin-3 in other tissues. Proteins were harvested from tissues of both male and female WT and Nucling$^{-/-}$ mice. The expression of galectin-3, as compared with that observed in the preputial gland, was up-regulated in the heart (Figure 7, lanes 1–4), lung (lanes 5–8), kidney (lanes 9–12), ovary (lanes 13 and 14) and testis (lanes 15 and 16) of Nucling$^{-/-}$ mice.

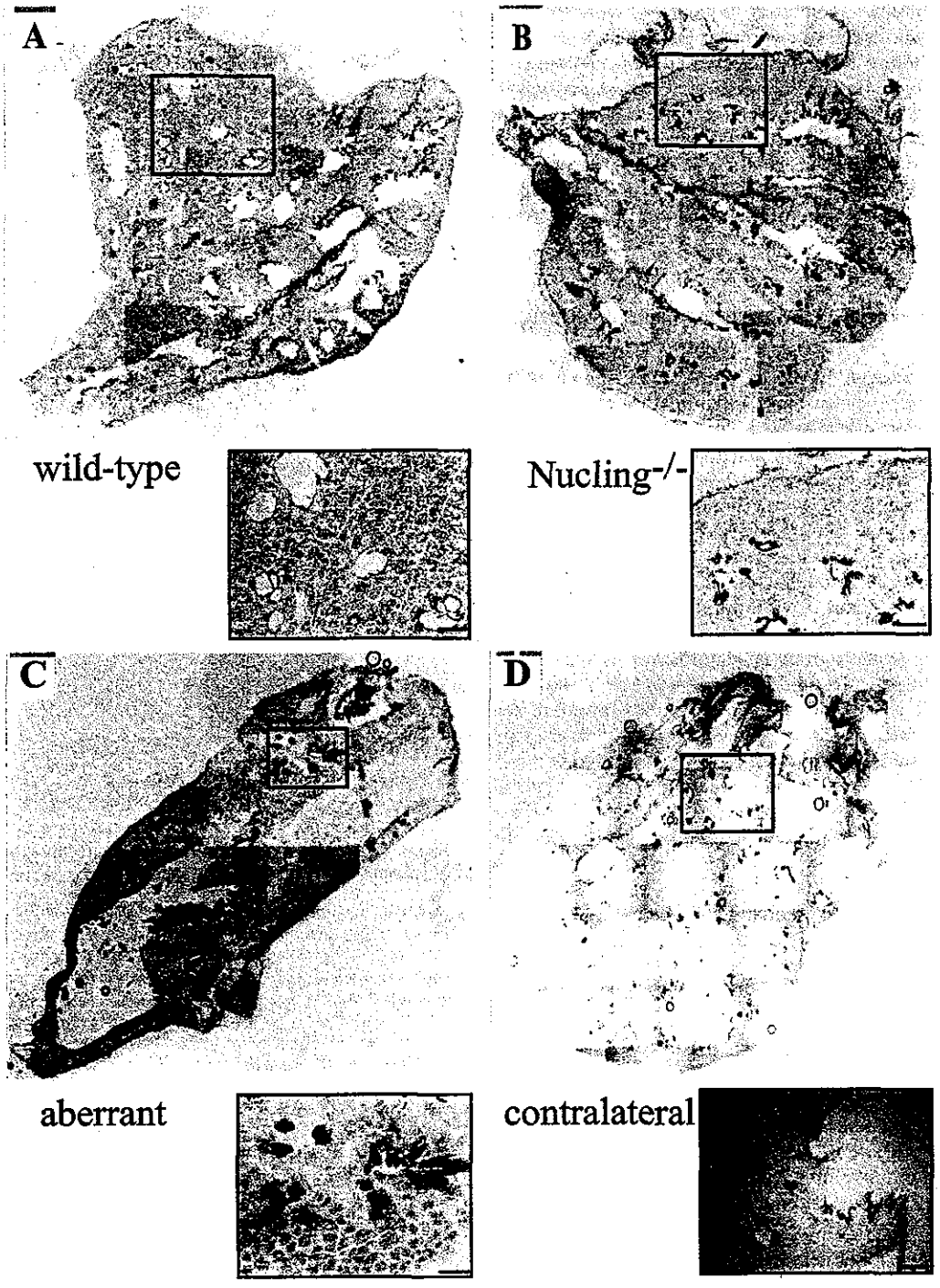


**Figure 5 Immunohistochemical analysis of up-regulation of galectin-3 in preputial gland of Nucling-null mice**

(**A–D**) Immunohistochemical localization of galectin-3 in preputial gland sections. Samples were obtained from 20-month-old WT mice (**A**), Nucling$^{-/-}$ mice (**B**) and abnormal Nucling$^{-/-}$ mice, including the aberrant side (**C**) and the contralateral side (**D**). *Frozen sections* were probed with Mac-2 antibody. Original magnification × 50.

## DISCUSSION

In the present study, two major targets have been achieved: that is, the identification of galectin-3 as a protein interacting with Nucling and a pathophysiological analysis of Nucling-deficient mice. $\beta$CAP73 was shown to interact with $\beta$-actin [2]. Since we used NuclingΔN as 'bait' to screen for the protein interacting with Nucling, $\beta$-actin may not be detected as positive clones by the yeast two-hybrid system in our study. However, galectin-4 was found to interact strongly with this bait. The interaction was confirmed further by immunoprecipitation assay (Figure 1B). In this assay, the binding capacity of NuclingΔN for galectin-4 was greater than that of full-length Nucling, supporting further the validity of using NuclingΔN as the bait (Figure 1B). In addition, several clones were identified which interact with Nucling, and some of them have been reported to be involved in apoptosis

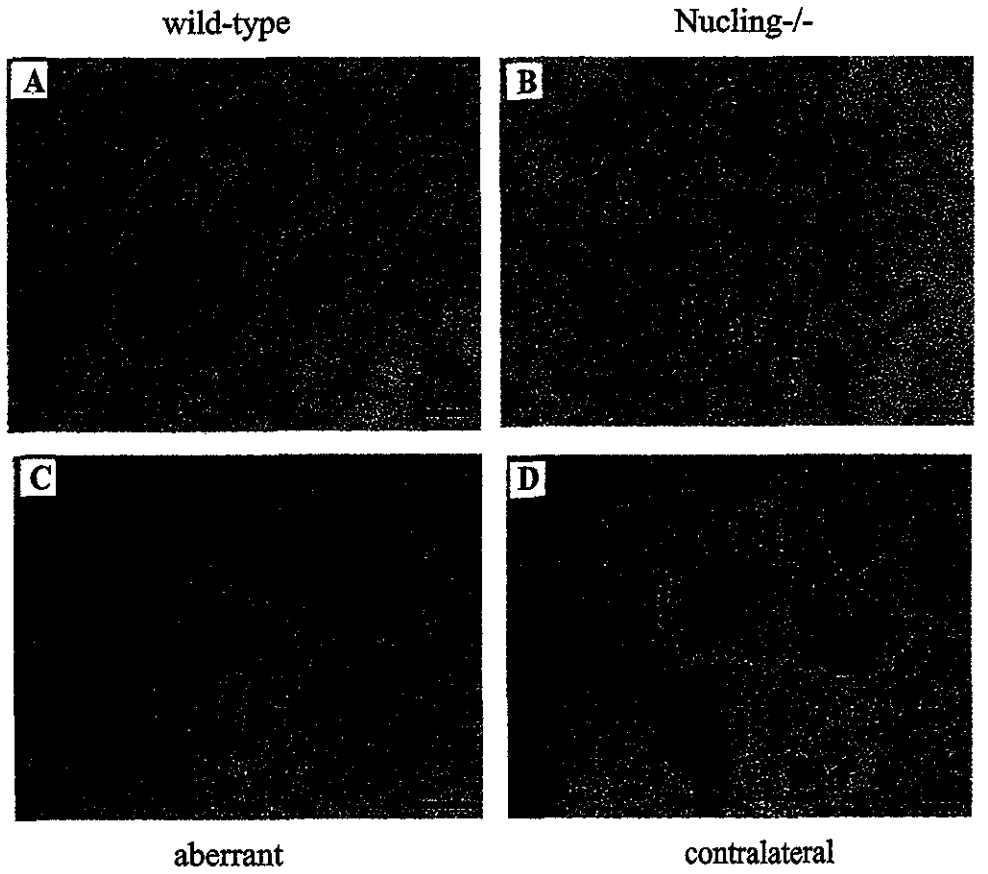


**Figure 6 Detection of apoptotic cells around luminal ducts of the preputial gland**

(**A**) Luminal ducts of the preputial gland in WT mice. (**B**) Luminal ducts of the preputial gland in Nucling$^{-/-}$ mice. (**C**) Aberrant side of the abnormal Nucling$^{-/-}$ preputial gland. (**D**) Contralateral side of the abnormal Nucling$^{-/-}$ preputial gland. Original magnification × 200.

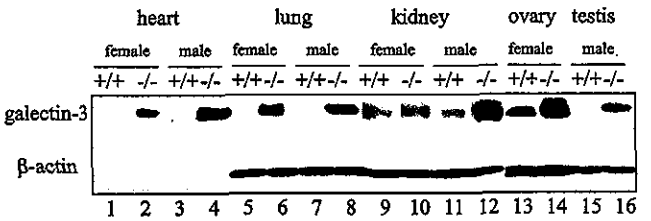


**Figure 7 Expression of galectin-3 is generally up-regulated in tissues of Nucling-null mice**

Extracted proteins from the heart (lanes 1–4), lung (lanes 5–8), kidney (lanes 9–12), ovary (lanes 13 and 14) and testis (lanes 15 and 16) were analysed by immunoblotting. Galectin-3 level in these tissues was examined with Mac-2 antibody. The same blot was probed with β-actin antibody (Sigma). This antibody does not stain adult cardiac and skeletal muscles.

(results not shown). Nucling was found to induce cytochrome *c* release, up-regulate Apaf-1 expression and recruit the Apaf-1–pro-caspase-9 complex for the induction of apoptosis following pro-apoptotic stress (T. Sakai, L. Liu, R. Mukai-Sakai, X. C. Teng, T. Mitani, M. Matsumoto, K. Toida, K. Ishimura, Y. Shishido, T. W. Mak and K. Fukui, unpublished work). In the present study, we have shown that Nucling-deficient cells are resistant to apoptosis (Figure 6B). These findings support further the pro-apoptotic role of Nucling. In addition, galectin-3 was demonstrated to interact with Nucling (Figure 1B). It is now well documented that galectin-3 has a critical role in the inhibition of apoptosis [9,10,17–20]. However, the signal transduction mechanism(s) of galectin-3 in relation to apoptosis is poorly understood. In the present study, we have shown that galectin-3 may negatively regulate apoptosome-dependent apoptosis by interacting with Nucling, a novel pro-apoptotic molecule.

It has been reported that NF-κB is involved in the regulation of galectin-3 expression [22]. We also found an NF-κB binding sequence (5′-GGGAGATCCC-3′) in the genomic sequence of Mac-2. We then showed that Nucling may inhibit NF-κB activation by interfering with the nuclear translocation of NF-κB–p65 from the cytoplasm (Figures 2D and 2E). The molecular mechanism underlying this regulatory role of Nucling in NF-κB activation remains to be investigated; however, the presence of the ankyrin repeat domain in both NF-κB [37] and Nucling may indicate the interaction of these molecules. In contrast with NF-κB-p65, the DNA-binding capacity of the NF-κB–p50 complex was lower in Nucling-deficient MEF nuclear extracts than that in Nucling$^{+/+}$ MEFs (Figure 2E, lanes 2 and 3, arrow B). Further detailed studies are necessary to analyse the precise mechanism of how Nucling regulates the NF-κB complexes containing p50 and p65 subunits. Taken all together, we postulate a distinct functional role of Nucling in the signalling pathway to apoptosis, as shown in Scheme 1.

The histopathological examination of Nucling-deficient mice revealed that preputial gland inflammatory lesions were found in more than 50% of the Nucling$^{-/-}$ mice from our production colonies under specific pathogen-free conditions (Table 1).

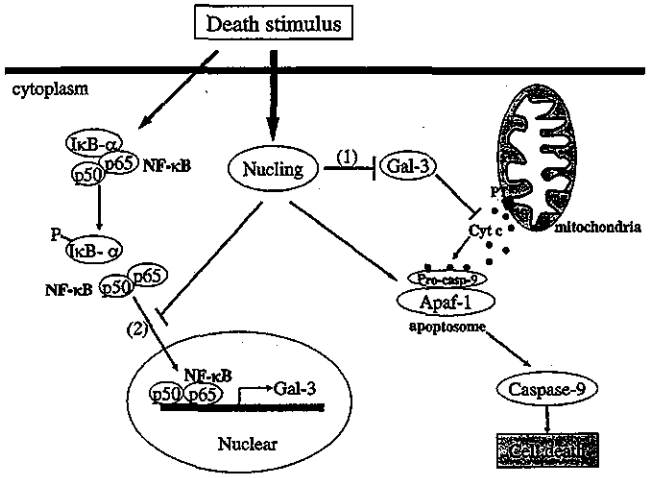


**Scheme 1 A possible pathway for the control of apoptosis involving *Nucling*, galectin-3 and NF-κB**

The Figure shows that: (1) Nucling directly interacts with galectin-3; and (2) Nucling interferes with NF-κB activity through preventing the nuclear translocation of the NF-κB–p65 complex from the cytoplasm.

Interestingly, galectin-3 expression was up-regulated in swollen preputial glands from Nucling$^{-/-}$ mice (Figures 4B, 5C and 5D). It has been reported that galectin-3 may be secreted through a classical or non-classical secretory route under inflammatory conditions [38–40], and may function in activating various cells regulating cell adhesion, attracting inflammatory cells to the site of inflammation [41]. NF-κB is also reported to be involved in inflammatory responses. We considered that NF-κB may be a key mediator in the regulation of galectin-3 and inflammatory responses in Nucling-deficient mice, and increased galectin-3 expression is tightly correlated with a longer duration of inflammatory lesions.

In addition, galectin-3 was localized around the luminal ducts in the preputial gland of Nucling$^{-/-}$ mice (Figures 5B–5D), in which impaired apoptosis was detected (Figures 6B–6D). Our results are in agreement with those of Harjacek et al. [35], who showed that increased galectin-3 expression is correlated with defective mononuclear cell apoptosis in patients with JIA. Therefore we conclude that galectin-3-induced defective apoptosis is one of the key processes leading to inflammation of the preputial gland in Nucling$^{-/-}$ mice.

On the other hand, there are reports suggesting that apoptosis is an important mechanism in ductal morphogenesis [42], and that p53-independent apoptosis is primarily involved in the formation of ducts [43]. In addition, the formation of vascular-like structures requires apoptotic cell death through the activation of a caspase-dependent mechanism and mitochondrial cytochrome *c* release [44]. However, it is not yet fully explained which apoptotic pathway regulates the formation of the ducts. In our study, apoptosis-positive and galectin-3-positive cells accumulated around the luminal ducts in the preputial gland (Figures 5B–5D, and Figure 6A), and the number of ducts in the gland was also decreased, as shown in Figures 3(F) and 3(G). These findings seem to imply that Nucling-induced apoptosis plays an important role in the formation of luminal ducts to maintain the function of the preputial gland.

Regarding the phenotype of Nucling$^{-/-}$ mice other than the inflammatory lesions in the preputial gland, mutant mice displayed no defects that were similar to those of Apaf-1$^{-/-}$ [45] or caspase-9$^{-/-}$ mice [46], including forebrain hyperplasia and embryonic lethality. Although this phenotypic discrepancy might come from the existence of unknown redundant molecules or pathways, it is not clear at present whether Nucling is an essential molecule or not for apoptosis pathways during development. These studies are currently under investigation.

We thank T. Nakamura for the plasmid containing galectin-1 and -3 cDNA. We are grateful to K. Irimura for H/E immunostaining and M. Shono for assistance with confocal microscopy. We also thank J. Yamada for technical support. This work was supported by a Grant-in-Aid for Scientific Research and a grant for the 21st Century COE Program from the Ministry of Education, Science, Sports and Culture of Japan, and by a Scientific Research grant from the Japan Society for the Promotion of Science. L. L. is supported by the Rotary-Yoneyama Memorial Foundation.

## REFERENCES

1 Sakai, T., Liu, L. and Fukui, K. (2003) Identification of a novel, embryonal carcinoma cell-associated molecule, Nucling, that is upregulated during cardiac muscle differentiation. J. Biochem. (Tokyo) **133**, 429–436
2 Welch, A. Y. and Herman, I. M. (2002) Cloning and characterization of CAP73, a novel regulator of β-actin assembly. Int. J. Biochem. Cell Biol. **34**, 864–881
3 Barondes, S. H., Cooper, D. N., Gitt, M. A. and Leffler, H. (1994) Galectins. structure and function of a large family of animal lectins. J. Biol. Chem. **269**, 20807–20810
4 Hirabayashi, J. and Kasai, K. (1993) The family of metazoan metal-independent β-galactoside-binding lectins: structure, function and molecular evolution. Glycobiology **3**, 297–304
5 Liu, F. T. (1993) S-type mammalian lectins in allergic inflammation. Immunol. Today **14**, 486–490
6 Flotte, T. J., Springer, T. A. and Thorbecke, G. J. (1983) Dendritic cell and macrophage staining by monoclonal antibodies in tissue sections and epidermal sheet. Am. J. Pathol. **111**, 112–124
7 Liu, F. T., Hsu, D. K., Zuberi, R. I., Kuwabara, I., Chi, E. Y. and Henderson, Jr, W. R. (1995) Expression and function of galectin-3, a β-galactoside-binding lectin, in human monocytes and macrophages. Am. J. Pathol. **147**, 1016–1028
8 Joo, H. G., Goedegebuure, P. S., Sadanaga, N., Nagoshi, M., von Bernstorff, W. and Eberlein, T. J. (2001) Expression and function of galectin-3, a β-galactoside-binding protein in activated T lymphocytes. J. Leukoc. Biol. **69**, 555–564
9 Kim, H.-R. C., Lin, H. M., Biliran, H. and Raz, A. (1999) Cell cycle arrest and inhibition of anoikis by galectin-3 in human breast epithelial cells. Cancer Res. **59**, 4148–4154
10 Matarrese, P., Fusco, O., Tinari, N., Natoli, C., Liu, F. T., Semeraro, M. L., Malorni, W. and Iacobelli, S. (2000) Galectin-3 overexpression protects from apoptosis by improving cell adhesion properties. Int. J. Cancer **85**, 545–554
11 Dagher, S. F., Wang, J. L. and Patterson, R. J. (1995) Identification of galectin-3 as a factor in pre-mRNA splicing. Proc. Natl. Acad. Sci. U.S.A. **92**, 1213–1217
12 Lin, H. M., Moon, B. K., Yu, F. and Kim, H.-R. C. (2000) Galectin-3 mediates genistein-induced $G_2$/M arrest and inhibits apoptosis. Carcinogenesis **21**, 1941–1945
13 Nangia-Makker, P., Honjo, Y., Sarvis, R., Akahani, S., Hogan, V., Pienta, K. J. and Raz, A. (2000) Galectin-3 induces endothelial cell morphogenesis and angiogenesis. Am. J. Pathol. **156**, 899–909
14 Song, Y. K., Billiar, T. R. and Lee, Y. J. (2002) Role of galetin-3 in breast cancer metastasis. Am. J. Pathol. **160**, 1069–1075
15 Honjo, Y., Nangia-Makker, P., Inohara, H. and Raz, A. (2001) Down-regulation of galectin-3 suppresses tumorigenicity of human breast carcinoma cells. Clin. Cancer Res. **7**, 661–668
16 Liu, F. T., Patterson, R. J. and Wang, J. L. (2002) Intracellular function of galectins. Biochim. Biophys. Acta **1572**, 263–273
17 Moon, B. K., Lee, Y. J., Battle, P., Jessup, J. M., Raz, A. and Kim, H.-R. C. (2001) Galectin-3 protects human breast carcinoma cells against nitric oxide-induced apoptosis. Am. J. Pathol. **159**, 1055–1060
18 Yang, R. Y., Hsu, D. K. and Liu, F. T. (1996) Expression of galectin-3 modulates T-cell growth and apoptosis. Proc. Natl. Acad. Sci. U.S.A. **93**, 6737–6742
19 Hsu, D. K., Yang, R. Y., Pan, Z. X., Yu, L., Salomon, D. R., Fung-Leung, W. P. and Liu, F. T. (2000) Targeted disruption of the galectin-3 gene results in attenuated peritoneal inflammatory responses. Am. J. Pathol. **156**, 1073–1083
20 Akahani, S., Nangia-Makker, P., Inohara, H., Kim, H.-R. C. and Raz, A. (1997) Galectin-3: a novel antiapoptotic molecule with a functional BH1 (NWGR) domain of bcl-2 family. Cancer Res. **57**, 5272–5276
21 Yu, F., Finley, Jr, R. L., Raz, A. and Kim, H.-R. C. (2002) Galectin-3 translocates to the perinuclear membranes and inhibits cytochrome c release from the mitochondria. J. Biol. Chem. **277**, 15819–15827
22 Dumic, J., Lauc, G. and Flogel, M. (2000) Expression of galectin-3 in cells exposed to stress – roles of jun and NF-κB. Cell Physiol. Biochem. **10**, 149–158

23 Baldwin, A. S. (1996) The NF-κB and I κB proteins: new discoveries and insights. Annu. Rev. Immunol. **14**, 649–683
24 Baichwal, V. R. and Baeuerle, P. A. (1997) Activate NF-κB or die? Curr. Biol. **7**, R94–R96
25 Baeuerle, P. A. and Henkel, T. (1994) Function and activation of NF-κB in the immune system. Annu. Rev. Immunol. **12**, 141–179
26 Beg, A. A. and Baltimore, D. (1996) An essential role for NF-κB in preventing TNF-α-induced cell death. Science **274**, 782–784
27 Perillo, N. L., Pace, K. E., Seilhamer, J. J. and Baum, L. G. (1995) Apoptosis of T cells mediated by galectin-1. Nature (London) **378**, 736–739
28 Matarrese, P., Tinari, N., Semeraro, M. L., Natoli, C., Iacobelli, S. and Malorni, W. (2000) Galectin-3 overexpression protects from cell damage and death by influencing mitochondrial homeostasis. FEBS Lett. **473**, 311–315
29 Rosenberg, L. M., Lyer, R., Cherayil, B., Chiodino, C. and Pillai, S. (1993) Structure of the murine Mac-2 gene. J. Biol. Chem. **268**, 12393–12400
30 Merkx, J., Solb, A. K. and van der Werff ten Bosch, J. J. (1988) The role of the preputial glands in sexual attractivity of the female rat. Physiol. Behav. **42**, 59–64
31 Colnot, C., Ripoche, M. A., Milon, G., Montagutelli, X., Crocker, P. R. and Poirier, F. (1998) Maintenance of granulocyte numbers during acute peritonitis is defective in galectin-3-null mutant mice. Immunology **94**, 290–296
32 Nishiyama, J., Kobayashi, S., Ishida, A., Nakabayashi, I., Tajima, O., Miura, S., Katayama, M. and Nogami, H. (2000) Up-regulation of galectin-3 in acute renal failure of the rat. Am. J. Pathol. **157**, 815–823
33 Nachtigal, M., Al-Assaad, Z., Mayer, E. P., Kim, K. and Monsigny, M. (1998) Galectin-3 expression in human atherosclerotic lesions. Am. J. Pathol. **152**, 1199–1208
34 Walther, M., Kuklinski, S., Pesheva, P., Guntinas-Lichius, O., Angelov, D. N., Neiss, W. F., Asou, H. and Probstmeier, R. (2000) Galectin-3 is upregulated in microglial cells in response to ischemic brain lesions, but not to facial nerve axotomy. J. Neurosci. Res. **61**, 430–435
35 Harjacek, M., Diaz-Cano, S., De Miguel, M., Wolfe, H., Maldonado, C. A. and Rabinovich, G. A. (2001) Expression of galectin-1 and -3 correlates with defective mononuclear cell apoptosis in patients with juvenile idiopathic arthritis. J. Rheumatol. **28**, 1914–1922
36 Iacobini, C., Amadia, L., Oddi, G., Ricci, C., Barsotti, P., Missori, S., Sorcini, M., Mario, U. D., Pricci, F. and Pugliese, G. (2003) Role of galectin-3 in diabetic nephropathy. J. Am. Soc. Nephrol. **14**, 264–270
37 Lank, V., Kourilsky, P. and Israel, A. (1992) NF-κB and related proteins: Rel/dorsal homologies meet ankyrin-like repeats. Trends Biochem. Sci. **17**, 135–140
38 Mehul, B. and Hughes, R. C. (1997) Plasma membrane targetting, vesicular budding and release of galectin-3 from the cytoplasm of mammalian cells during secretion. J. Cell. Sci. **110**, 1169–1178
39 Menon, R. P. and Hughes, R. C. (1999) Determinants in the N-terminal domains of galectin-3 for secretion by a novel pathway circumventing the endoplasmic reticulum-Golgi complex. Eur. J. Biochem. **264**, 569–576
40 Nickel, W. (2003) The mystery of non-classical protein secretion. Eur. J. Biochem. **270**, 2109–2119
41 Liu, F. T. (2000) Galectins: a new family of regulators of inflammation. Clin. Immunol. **97**, 79–88
42 Abe, K. and Watanabe, S. (1995) Apoptosis of mouse pancreatic acinar cells after duct ligation. Arch. Histol. Cytol. **58**, 221–229
43 Humphreys, R. C., Krajewska, M., Krnacik, S., Jaeger, R., Weiher, H., Krajewski, S., Reed, J. C. and Rosen, J. M. (1996) Apoptosis in the terminal endbud of the murine mammary gland: a mechanism of ductal morphogenesis. Development **122**, 4013–4022
44 Segura, I., Serrano, A., De Gonzalez, G. G., Gonzalez, M. A., Abad, J. L., Claveria, C., Gomez, L., Bernad, A., Martinez-A, C. and Riese, H. H. (2002) Inhibition of programmed cell death impairs *in vitro* vascular-like structure formation and reduces *in vivo* angiogenesis. FASEB J. **16**, 833–841
45 Cecconi, F., Alvarez-Bolado, G., Meyer, B. I., Roth, K. A. and Gruss, P. (1998) Apaf1 (CED-4 homolog) regulates programmed cell death in mammalian development. Cell **94**, 727–737
46 Hakem, R., Hakem, A., Duncan, G. S., Henderson, J. T., Woo, M., Soengas, M. S., Elia, A., Pompa, J. L., Kagi, D., Khoo, W. et al. (1998) Differential requirement for caspase 9 in apoptotic pathways *in vivo*. Cell **94**, 339–352

Received 26 August 2003/16 December 2003; accepted 13 February 2004
Published as BJ Immediate Publication 13 February 2004, DOI 10.1042/BJ20031300

行なう生産性の高い植物の作出のために，$CO_2$ 認識能に優れ，反応速度の高い RuBisCO の分子育種が求められているが，試験管内分子進化研究から得られる情報は RuBisCO の分子育種のための大きなヒントになるだろう．

1) F.C. Hartman & M.R. Harpel：*Annu. Rev. Biochem.*, 63, 197 (1994).
2) 横田明穂："植物分子生理学入門"，学会出版センター，1999, p.81.
3) H. Ashida, Y. Saito, C. Kojima, K. Kobayashi, N. Ogasawara & A. Yokota：*Science*, 302, 286 (2003).

(蘆田弘樹[*1]，横田明穂[*2]，[*1]オーストラリア国立大学生物科学研究部，[*2]奈良先端科学技術大学院大学バイオサイエンス研究科)

# D-アミノ酸バイオシステムによる哺乳類の中枢神経機能の制御

## 脳内在性 D-セリンと D-アミノ酸酸化酵素の役割

生体を構成する 20 種類のアミノ酸のうち不斉炭素原子をもつアミノ酸には，互いに鏡像関係にある 2 種類の光学異性体（D 型，L 型）が存在する．D-アミノ酸酸化酵素（EC 1.4.3.3）はこれら 2 種類の光学異性体のうち，D 型のアミノ酸のみを特異的に酸化することで知られている．筆者らは，中枢神経系における D-アミノ酸代謝機構の解明を目的として，グルタミン酸受容体サブタイプである NMDA（*N*-methyl-D-aspartate）受容体の機能不全に由来する難治性精神疾患や，さらには脳卒中における神経細胞死に対する新規治療薬開発に向けて，多角的なアプローチに基づく解析を進めている．

D-アミノ酸酸化酵素は，その活性中心に補酵素として FAD (flavin adenine dinucleotide，ビタミン $B_2$ として知られるリボフラビンの誘導体）をもつフラビン酵素で，D-アミノ酸の中でも特に中性および芳香族性のものを良い基質とするが，グリシンやサルコシンも基質となり得る[(1)]．一方，D-グルタミン酸は酸化されず，D-アスパラギン酸に対しては独立に，D-アスパラギン酸オキシダーゼ（EC 1.4.3.1）が存在する．反応は，下式に示すように，FAD が還元的半反応により還元型

$$RCHNH_2COOH + EFAD \rightleftharpoons RC{=}NHCOOH + EFADH_2$$
$$RC{=}NHCOOH + H_2O \rightleftharpoons RCOCOOH + NH_3$$
$$EFADH_2 + O_2 \longrightarrow EFAD + H_2O_2$$

E は酵素

となり，同時にアミノ酸が酸化されてイミノ酸となる．生じたイミノ酸は加水分解により $\alpha$-ケト酸とアンモニアとなる．還元型 FAD は，酸化的半反応により酸化型に戻り，過酸化水素を生じる．本酵素の C 末端には，3 残基のアミノ酸（Ser-His-Leu）からなるペルオキシソーム移行シグナル（PTS 1；peroxisome targeting signal 1）が存在するため，本酵素は細胞質で生合成された後，細胞内小器官の一つであるペルオキシソームに移行・局在する．アミノ酸の代謝によって生じた過酸化水素は，カタラーゼなどによって分解される．

本酵素は，1935 年にクエン酸回路で知られる Krebs によって発見されて以来[(2)]，その反応機構について詳細な解析がなされてきた[(3)]．現在知られている 800 種類以上のフラビン酵素の中でも最も長い研究の歴史をもっている．しかし，L 型のアミノ酸のみで構成されると考えられていた生体において，D 型のアミノ酸を酸化する本酵素が，腎臓や肝臓，そして脳に存在する意義については，長い間不明とされてきた．ところが近年，本酵素の生理的役割を示唆するデータが蓄積されるにつれ，本酵素の"中枢神経系における神経伝達制御因子"としての認識が高まり，2004 年現在，統合失調症など難治性精神疾患の病態解明，および新規治療薬開発の可能性からも，本酵素を中心とした D-アミノ酸バイオシステムの研究が脚光を浴びている．

生体内における本酵素の生理的基質は従来不明とされてきたが，1993 年に西川らにより，ラット脳において D-セリンが高濃度に存在し，その中枢神経系における分布が NMDA 受容体の分布と一致することが示された[(4)]．さらに 1995 年には，Snyder らにより，D-セリンが NMDA 受容体のグリシン結合部位における選択的アゴニストとして作用することが見いだされ，D-セリンの"中枢神経系における神経調節因子"としての存在意義が示唆された[(5)]．Snyder らはまた 1999 年に，中枢神経系において L-セリンから新たに D-セリンを生合成する酵素として，セリンラセマーゼを同定・報告している．こうして D-セリンは，生合成酵素としてのセリンラセマーゼと，分解酵素としての D-アミノ酸酸化酵素とともに，"NMDA 受容体を介する興奮性神経伝達における

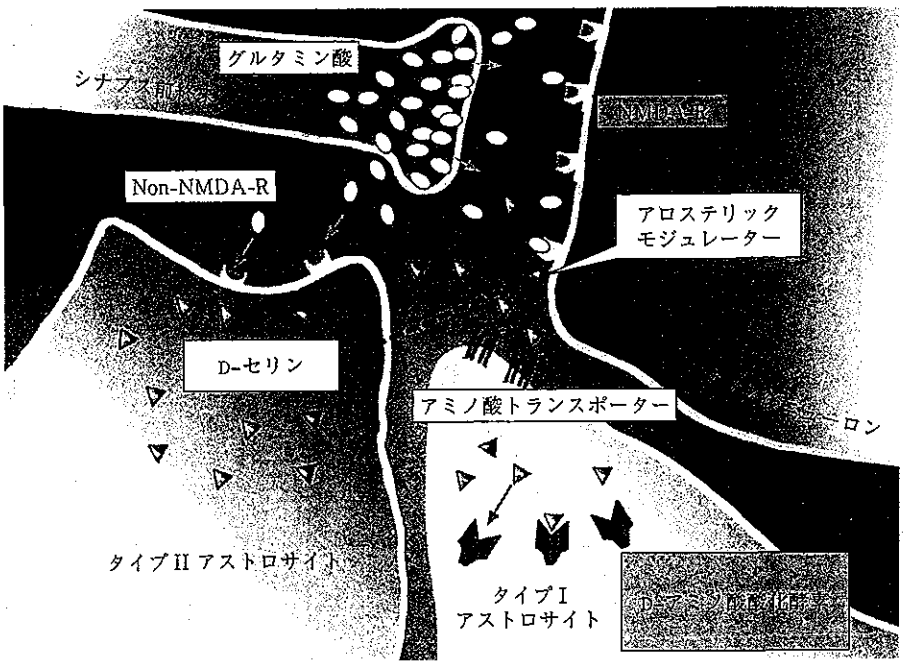


**図 1 ■ 中枢神経系「D-セリン/D-アミノ酸酸化酵素システム」のモデル**

D-セリン生合成の場としてのタイプII アストロサイト，およびD-セリン代謝の場としてのタイプI アストロサイトを示す．D-セリンはグルタミン酸ニューロンの神経伝達において，アロステリックにNMDA 受容体に作用し，神経調節因子として働く．D-アミノ酸酸化酵素は中枢神経系においてこの調節因子としてのD-セリンの濃度を制御していると考えられる．NMDA-R：*N*-methyl-D-aspartate 受容体

神経調節因子" としての地位を確立するに至った．

こうしたD-アミノ酸バイオシステム新生の流れの中で，筆者らは，D-アミノ酸酸化酵素遺伝子のクローニングを行ない，ブタ (1987)，ヒト (1988)，マウス (1990)，ウサギ (1990) のcDNA とヒトゲノム遺伝子を単離・同定することに成功している[6]．さらに，中枢神経系においてD-セリンを代謝・制御する因子として本酵素に着目し，本酵素遺伝子の脳特異的発現を明らかにしてきた．特に，D-セリンと本酵素の中枢神経系における分布が負の相関を示すことから，D-セリンを本酵素の内在性基質と位置づけ，「本酵素は中枢神経系において，D-セリンを介したNMDA 受容体の神経伝達を制御する因子である」 との概念を提唱している．筆者らはすでに，ラット脳よりグリア細胞の初代培養系を確立し，本酵素の遺伝子発現を，小脳のみならず，従来は否定的であった大脳由来のグリア細胞においても確認した．さらに，タイプI，タイプIIアストロサイト（星状膠細胞）の分離培養を行ない，D-セリン産生の場が主にタイプIIアストロサイトであるのに対し，本酵素の発現はタイプI アストロサイトにおいて顕著であることを示した[7]．これらの知見に基づき，グルタミン酸ニューロンにおける "D-セリン/D-アミノ酸酸化酵素システム" の機能についてモデル化したものが図1である．

2002 年には，Chumakov らのゲノム解析により，統合失調症の疾患感受性遺伝子として，本酵素と本酵素の活性化因子としての新規遺伝子 G72 が報告された[8]．これは，「本酵素活性の上昇が中枢神経系における神経調節因子としてのD-セリン濃度の低下を招き，NMDA 受容体の機能不全に由来する統合失調症の発症とその病態に関係する」との仮説を強く裏づけるものである．現在は，中枢神経系発生過程での本酵素機能の解析，中枢神経系D-セリン合成・代謝系の解明に向けたプロテオーム解析，X 線立体構造解析に基づくヒト酵素特異的な阻害剤探索を目指し，解析を進めている．特にヒト酵素の結晶構造解析は，将来中枢神経系におけるD-セリン代謝系および統合失調症発症の分子機構が明らかになった際に，新規治療薬開発に対する分子的基盤を与えるものであり，生化学的な重要性のみならず，医学的応用面においてもその成果が期待されている．

1) 三宅可浩，福井　清："廣川 タンパク質化学 第4巻"，廣川書店，2000，p.87.
2) H.A. Krebs：*Biochem. J.*, 29, 1620 (1935).
3) B. Curti, S. Ronchi & M.P. Simonetta："Chemistry and Biochemistry of Flavoenzymes", Vol. III, CRC Press, 1992, p.69.
4) A. Hashimoto, T. Nishikawa, T. Oka & K. Takahashi：*J. Neurochem.*, 60, 783 (1993).
5) M.J. Schell, M.E. Molliver & S.H. Snyder：*Proc. Natl. Acad Sci. USA*, 92, 3948 (1995).
6) K. Fukui & Y. Miyake：*J. Biol. Chem.*, 267, 18631 (1992).
7) Y. Urai, O. Jinnouchi, K.T. Kwak, A. Suzue, S. Nagahiro

& K. Fukui : *Neurosci. Lett.*, 324, 101 (2002).
8) I. Chumakov *et al.* : *Proc. Natl. Acad. Sci. USA*, 99, 13675 (2002).

(川添僚也，小野公嗣，朴　煥埼，頼田和子，冨田優美子，福井　清，徳島大学分子酵素学研究センター，大学院医学研究科)

# ヘム鉄の酸化⇄還元を利用する分子センサータンパク質
## 結晶構造解析が解き明かす分子スイッチの制御機構

微生物からヒトに至るまで，生物は様々な環境変化への応答機構をもっている．たとえば，微生物は栄養物質の濃度に応答して鞭毛の回転を制御する走化性と呼ばれる機構を有しており，また植物は光環境に応じて細胞内の葉緑体の位置を変化させ，光合成効率を最適に保つ機構を備えている．このような物理化学的な環境変化を検出し，適切な細胞シグナルへと変換しているのは，センサータンパク質と呼ばれる多様なタンパク質群である．

これらのセンサータンパク質は一般に，センサードメインと，細胞シグナルを伝達するエフェクタードメインからなる（図1）．まず，センサードメインはレドックス（redox，酸化還元），酸素，光などの環境変化を入力信号として感知し，その立体構造を変化させる．これによってエフェクタードメインとの相互作用が変化し（細胞内シグナル伝達），最終的にはエフェクタードメインの酵素活性を制御し，環境変化に対応するための様々な細胞シグナルを出力するのである．

最近，ヘムタンパク質の中にも，従来からよく知られている酸素運搬（ヘモグロビン），電子伝達（シトクローム）および酸素原子添加酵素（P450）といった機能とは別に，センサーとして働くタンパク質が次々と発見され注目を浴びている．これらのヘムセンサータンパク質ファミリーには，NOセンサーである可溶性グアニル酸シクラーゼ，COセンサー転写因子であるCooA，生物時計に関わるCOセンサー転写因子NPAS2，根粒菌の窒素固定に関わる酸素センサーFixL，古細菌の走化性に関わる酸素センサーHemeATなどが含まれる[1,2]．これらのヘムセンサータンパク質が分子レベルでどのように環境変化を感知し，その情報をエフェクタードメインへと伝達しているかはまだ不明な部分が多く，タンパク質の三次元構造レベルでの詳細な解析が必要であった．

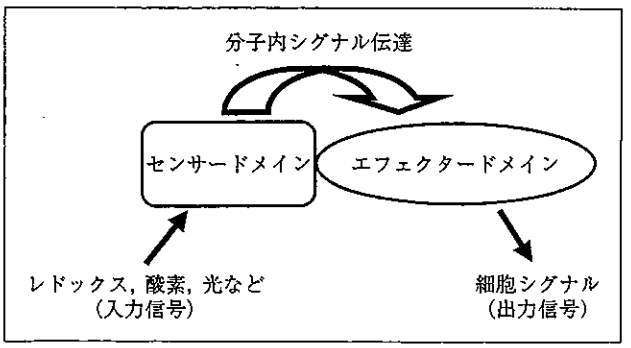


図1■センサータンパク質による細胞シグナル制御の模式図

筆者らの研究室では，大腸菌のヘムセンサータンパク質であるEcDOSに着目し，そのセンシング機構の詳細な解明を目指した研究を行なっている．EcDOSはFixL同様，PASと呼ばれるセンサータンパク質に多く見られる構造モチーフをもつヘム結合センサードメインと，微生物によく保存されたGGDEF，EALモチーフを含むホスホジエステラーゼドメインから構成されている[3,4]．全体のドメイン構造は酢酸菌のセルロース合成制御に関わるAxPDEA1という酵素とよく似ている．AxPDEA1はセルロース合成酵素の活性化に必要な環状ヌクレオチド（サイクリックジGMP）を酸素濃度に依存して分解するホスホジエステラーゼである．EcDOSについても同様に酸素センサーとして機能しているのではないかという提案がなされた[5]．しかし，ヘム配位子の結合速度の解析や，酸素結合体の安定性などから，むしろEcDOSは酸素センサーではなく，レドックスセンサーとして機能している可能性が示唆された[6]．筆者らは，cAMPを基質として用いたときにEcDOSがホスホジエステラーゼ活性を有することを見いだし，これをモデル系としてEcDOSの機能解析を行なった．その結果，EcDOSはヘム鉄が還元型のときにのみホスホジエステラーゼ活性を示し，ヘム鉄が酸化型のときは活性がみられなかった．また，COやNOがヘム鉄に結合しても，活性が阻害されることがわかった[4]．

Original Paper

European Neurology

Eur Neurol 2004;52:151–155
DOI: 10.1159/000081624

Received: December 8, 2003
Accepted: August 13, 2004
Published online: October 18, 2004

# Whole-Brain Voxel-Based Correlation Analysis between Regional Cerebral Blood Flow and Intelligence Quotient Score in Parkinson's Disease

Kenichi Oishi[a,b] Masafumi Ogawa[a] Yasushi Oya[a] Mitsuru Kawai[a]

[a]Department of Neurology, National Center Hospital for Mental, Nervous and Muscular Disorders, National Center of Neurology and Psychiatry, Kodaira, and [b]Division of Endocrinology/Metabolism, Neurology and Hematology/Oncology, Kobe University Graduate School of Medicine, Kobe, Japan

**Key Words**

Parkinson's disease · Cognitive impairment · Wechsler Adult Intelligence Scale, Revised · Intelligence quotient · Regional cerebral blood flow · Voxel-based analysis · Single-photon emission computed tomography

**Abstract**

The correlation between regional cerebral blood flow (rCBF) and intelligence quotient (IQ) score was investigated in patients with Parkinson's disease (PD) without severe dementia. We analyzed the $^{99m}$Tc-ethyl cysteinate dimer single-photon emission computed tomography quantitative images and Revised Wechsler Adult Intelligence Scale scores of 44 PD patients using statistical parametric mapping. Verbal IQ positively correlated with rCBF in the right ventral striatum and the bilateral prefrontal cortex, performance IQ positively correlated with rCBF in the right operculum, insula and the left middle temporal gyrus, and full-scale IQ positively correlated with rCBF in the right operculum, insula and the ventral striatum. The identified areas may be functionally related to mild to moderate cognitive impairment in patients with PD.



## Introduction

In patients with Parkinson's disease (PD), general intelligence, as estimated by the intelligence quotient (IQ) score of the Revised Wechsler Adult Intelligence Scale (WAIS-R), declines with disease progression [1, 2]. Neuropathologically, depletion of multiple neuronal networks [3] or cortical changes such as Lewy bodies [4] or Alzheimer-type lesions [5] may account for the decline in IQ, although the specific causal mechanism remains controversial [6]. The neuroradiological technique of comparing regional cerebral blood flow (rCBF) or metabolism to neuropsychological test performance is an approach that reveals the functional anatomy of the brain while overcoming the methodological limitations of analysis by autopsy. Hu et al. [7] performed the first study correlating brain metabolism at rest with IQ. The authors analyzed regions of interest based on an a priori hypothesis in nondemented PD patients using magnetic resonance spectroscopy and positron emission tomography (PET). They reported significant correlations between left temporoparietal hypometabolism and reductions in full-scale IQ (FSIQ) and verbal IQ (VIQ). They also found a significant correlation between right temporoparietal hypometabolism and reductions in performance IQ (PIQ). However,

KARGER
Fax + 41 61 306 12 34
E-Mail karger@karger.ch
www.karger.com


0014–3022/04/0523–0151$21.00/0

Accessible online at:
www.karger.com/ene

Kenichi Oishi, MD
Division of Endocrinology/Metabolism, Neurology and Hematology/Oncology
Kobe University Graduate School of Medicine
7-5-2 Kusunoki-cho, Chuo-ku, Kobe 650-0017 (Japan)
Tel. +81 78 382 5885, Fax +81 78 382 5899, E-Mail dfbyv904@kcc.zaq.ne.jp

due to technical limitations, large areas, including frontal areas of the brain, went unexplored. Impaired frontal function has been demonstrated both by neuropsychological tests [8, 9] and a PET study [10] in PD patients. Therefore, the purpose of the present study was to explore the anatomical background of IQ decline in PD by performing voxel-based whole-brain correlation analysis between rCBF and IQ score.

## Subjects and Methods

We retrospectively analyzed the clinical database of the $^{99m}$Tc-ethyl cysteinate dimer (ECD) single-photon emission computed tomography (SPECT) quantitative images and WAIS-R [11] scores of 44 PD patients (21 males and 23 females, age: mean 66 years, SD 8.4) admitted to the National Center Hospital for Mental, Nervous and Muscular Disorders from 1997 to 2000 for the diagnosis and/or treatment of PD. The mean duration of PD was 9.2 years (SD 7.4). PD was diagnosed if a patient had resting tremor, cogwheel rigidity and bradykinesia that were improved by levodopa or a dopamine receptor agonist. Brain MRI scans were performed in all subjects, and patients with brain atrophy, ischemia or hydrocephalus were excluded. No patient had apraxia, ataxia, dysarthria, hallucinations or a history of encephalitis. Patients with severe dementia, as defined by the Diagnostic and Statistical Manual of Mental Disorders, Third Edition Revised (DSM-III-R), were also excluded. All patients were right-handed. Eight patients were assessed as Hoehn-Yahr stage I, 10 as stage II, 17 as stage III and 9 as stage IV. Nineteen patients were predominantly symptomatic on the right side of the body, 19 patients on the left side, and 6 were bilaterally affected. Patients were medicated with various combinations of levodopa with a decarboxylase inhibitor and dopamine receptor agonists. Cognitive function was measured by the WAIS-R, but 3 patients in Hoehn-Yahr stage IV could not accomplish the performance subtest because of motor dysfunction due to PD. The mean VIQ was 90.6 (SD 14.8, range 59–121), the mean PIQ 87.8 (SD 14.8, range 59–119) and the mean FSIQ 89.0 (SD 14.8, range 65–121). Even patients with low IQ scores did not require continuous supervision in daily living and did not meet DSM-III-R criteria for severe dementia.

The $^{99m}$Tc-ECD SPECT images were routinely taken for clinical purposes to rule out parkinsonism secondary to other causes. Each patient received a 600-MBq intravenous injection of $^{99m}$Tc-ECD at rest. Ten minutes after the injection, brain SPECT was performed using a rectangular gamma camera with the parallel-hole collimator of the three-head SPECT system (Multispect3; Siemens Medical Systems, Hoffman Estates, Ill., USA). The projection data were obtained in a 128 × 128 format. Global CBF [12] and rCBF [13] were noninvasively measured as described above. The images were manipulated using Matlab (Mathworks, Sherborn, Mass., USA) and SPM99 software (Wellcome Department of Cognitive Neurology, UCL, London, UK). Each image was spatially normalized to the standardized brain template provided by the Montreal Neurological Institute, with further isotropic smoothing, to a total of 12 mm. The final image format was 16-bit, with a size of 79 × 95 × 68 and a voxel size of 2 × 2 × 2 mm. Global CBF for each subject was normalized to 50 ml/100 g/min with proportional scaling. Statistical correlations between rCBF and IQ subscores (VIQ, PIQ and FSIQ) were explored voxel by voxel using statistical parametric mapping, by setting each patient's IQ score as a covariate of interest. Significance was accepted if the clusters survived a corrected threshold of $p < 0.05$.

**Table 1.** Montreal Neurological Institute coordinates of local maxima for the rCBF significantly correlated with VIQ, PIQ and FSIQ ($p < 0.05$ at cluster level, corrected)

| Structure | Coordinates | | | Z score |
|---|---|---|---|---|
| | x | y | z | |
| VIQ | | | | |
| Right PFC | 16 | 62 | −4 | 4.24 |
| Right ventral striatum | 12 | 18 | −8 | 4.02 |
| Left PFC | −40 | 36 | 14 | 4.02 |
| PIQ | | | | |
| Right frontal operculum | 60 | 10 | 12 | 4.30 |
| Right insula | 40 | 8 | −2 | 4.20 |
| Left middle temporal gyrus | −60 | −20 | −10 | 4.24 |
| FSIQ | | | | |
| Right frontal operculum | 62 | 10 | 16 | 3.38 |
| Right insula | 36 | 12 | −4 | 3.76 |
| Right ventral striatum | 14 | 20 | −8 | 3.51 |

## Results

VIQ positively correlated with rCBF in the right ventral striatum and the bilateral prefrontal cortices (PFC), especially in the right Brodmann's area (BA) 10 and 8 and the left BA 46 (fig. 1 and table 1). PIQ correlated with rCBF to the right frontal operculum (BA 44, 6), the right insula and the left middle temporal gyrus (BA 21), and FSIQ correlated with rCBF to the right frontal operculum (BA 6), right ventral striatum and the right insula (fig. 1 and table 1). The correlation of the rCBF in the PFC and ventral striatum to VIQ scores is shown in figure 2. rCBF did not negatively correlate with VIQ, PIQ or FSIQ in any area.

## Discussion

The intellectual decline demonstrated by our subject population may be related to the statistically significant correlations we found between IQ scores and the rCBF of several brain regions. VIQ and PIQ scores correlated with rCBF in the PFC and ventral striatum. These areas contain the frontal-subcortical circuits [14] crucial for main-

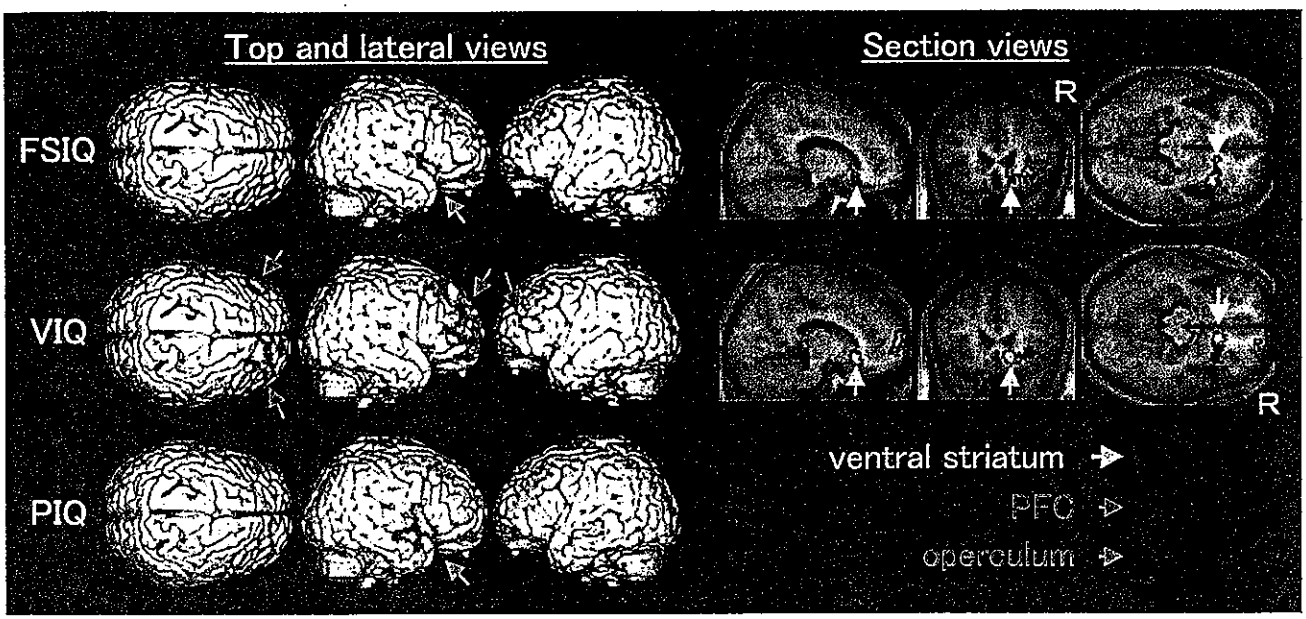


**Fig. 1.** rCBF significantly correlated with VIQ, PIQ and FSIQ ($p < 0.05$ at cluster level, corrected). rCBF in the ventral striatum, which is overlaid on the section views of the standardized magnetic resonance imaging template, is significantly correlated with VIQ and FSIQ. R = Right.

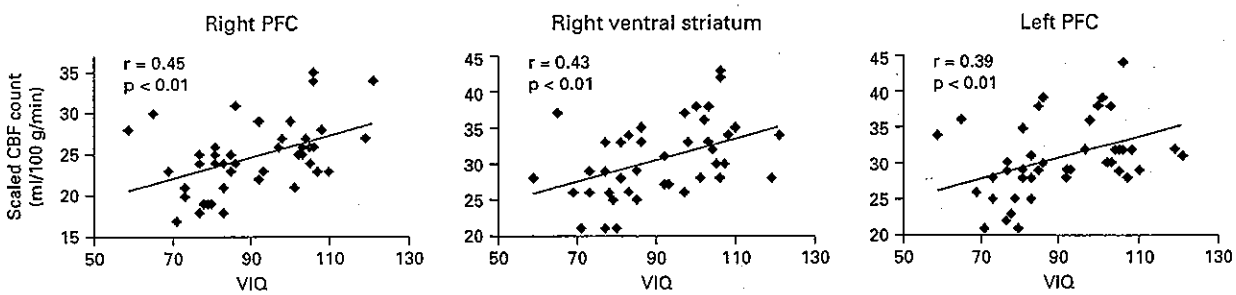


**Fig. 2.** The scaled rCBF in the local maxima of the right and left PFC and the ventral striatum are plotted against the VIQ score.

tenance and manipulation of information in working memory processes as well as for regulation of concentration, attention and motivation [15]. Depletion of these cognitive and affective functions is characteristic of PD [8, 9]; one possible explanation is that the dysfunction in the frontal-subcortical circuits causes IQ decline, especially in VIQ, which requires working memory and concentration [11]. Moreover, these areas receive dopaminergic projection from the ventral tegmental area [16, 17], which is known to deteriorate in PD [5]. Considering that patients with autosomal recessive juvenile parkinsonism associated with the *parkin* gene mutation without ventral tegmental area lesions do not suffer from dementia [18], degeneration of the ventral tegmental area may be one possible cause of the rCBF decline. We also found a positive correlation between PIQ scores and the rCBF in the right operculum and the insula, areas which are activated in normal subjects during executive tasks, including vi-

suospatial manipulation [19]. The rCBF decline in these areas may be one cause for the decline in PIQ, which requires visuospatial manipulation. Hu et al. [7] reported a similar correlation between the reduction in PIQ and the regional cerebral oxidative phosphorylation in a voxel of interests including the bilateral insula and operculum. However, due to technical limitations, they were unable to set the voxel of interest in the frontal lobe, where we found the correlation with VIQ. On the other hand, we did not find any correlation between FSIQ and VIQ scores and rCBF in the left temporoparietal areas. This may be due in part to the difference in modality between our two studies, as deficits in oxidative phosphorylation are perhaps more pertinent to cognitive function than deficits in glycolysis, which affects rCBF.

The WAIS-R is one of the most commonly used tests of general intelligence, with 6 verbal and 5 performance subtests. The FSIQ score may reflect a combination of cognitive deficits, but previous attempts to associate subtest performance with specific abnormalities or brain lesions have remained inconclusive. Several studies [20, 21] have demonstrated correlations between rCBF in the parietal lobe and general cognitive function in patients with Alzheimer's disease. One such study, involving a mixed subject population of normal and Alzheimer's disease patients, used fluorodeoxyglucose $^{18}$F-PET to localize VIQ-related brain activity to the left parasylvian area and PIQ activity to the right posterior parietal lesion [22]. However, we found no such correlations in our PD population. Therefore it seems that the anatomical lesions that contribute to IQ reduction may differ by the underlying disease process, at least in a comparison of Alzheimer's disease and PD.

In this study, we focused on IQ scores rather than on the specific cognitive functions, such as working memory or execution function, which typically decline in PD [8, 9, 23]. IQ scores are clinically used widely to assess intellectual function in many diseases. Moreover, it should be noted that the IQ score is not an index of 'purely cognitive' function, but rather reflects numerous aspects of mental activity [11]. As discussed above, our results suggested that the IQ reduction in PD is related to specific cognitive and affective alterations based on PD pathology, and that this background differs from that of AD. Affective alteration, in particular, may influence IQ scores in PD. Mentis et al. [24] investigated the topographic pattern of glucose metabolism at rest in relation to cognitive or mood alteration in PD without clinical dementia and depression, and found that hypometabolism in the lateral and medial frontal cortex correlated with mood alteration. We found an overlapping correlation between rCBF and FSIQ/VIQ in the same regions, suggesting that IQ reduction and affective alteration share a common pathophysiological background in PD.

Two limitations of the study design should be addressed. First, the lack of an appropriate control group limits the findings of the current study; whether the above correlations are specific to PD cannot be determined. Moreover, in the literature there are no studies of normal subjects that investigate the relationship between IQ and either rCBF or regional cerebral glucose metabolism at rest. In fact, little is known about the localization of intelligence in the normal brain, although several cognitive factors that characterize intellectual function have been elucidated by observing brain activation during specific task performance [25]. For instance, attention span, visuospatial abilities and problem-solving processes have been attributed to the right prefrontal regions [26, 27], parietal cortex [28, 29] and frontoparietal network [30, 31], respectively. However, the topographic pattern under activation conditions is different from the pattern evident in resting conditions, which is directly affected by the underlying pathological alteration [24]. Thus, future investigations ought to study the correlation between IQ and rCBF in normal subjects to confirm the PD-specific pathological mechanisms which underlie IQ decline.

Furthermore, the motor retardation characteristic of the PD population may confound results of the performance subtests, which are time-restricted and demand motor facility. However, the verbal subtests do not require motor ability beyond speech production.

In summary, the IQ decline experienced by patients with PD may be related to CBF in specific brain regions. Altered rCBF in these areas may reflect the pathological changes of the PD brain.

**Acknowledgements**

The authors thank Dr. Hiroshi Matsuda and Dr. Takashi Onishi (Department of Radiology, National Center Hospital for Mental, Nervous and Muscular Disorders, National Center of Neurology and Psychiatry, Kodaira, Japan) for image acquisition and helpful comments.